

A Generalized Adaptive Joint Learning Framework for High-Dimensional Time-Varying Models

Baolin Chen* Mengfei Ran†

January 9, 2026

Abstract

In modern biomedical and econometric studies, longitudinal processes are often characterized by complex time-varying associations and abrupt regime shifts that are shared across correlated outcomes. Standard functional data analysis (FDA) methods, which prioritize smoothness, often fail to capture these dynamic structural features, particularly in high-dimensional settings. This article introduces Adaptive Joint Learning (AJL), a regularization framework designed to simultaneously perform functional variable selection and structural changepoint detection in multivariate time-varying coefficient models. We propose a convex optimization procedure that synergizes adaptive group-wise penalization with fused regularization, effectively borrowing strength across multiple outcomes to enhance estimation efficiency. We provide a rigorous theoretical analysis of the estimator in the ultra-high-dimensional regime ($p \gg n$), establishing non-asymptotic error bounds and proving that AJL achieves the oracle property—performing as well as if the true active set and changepoint locations were known a priori. A key theoretical contribution is the explicit handling of approximation bias via undersmoothing conditions to ensure valid asymptotic inference. The proposed method is validated through comprehensive simulations and an application to Primary Biliary Cirrhosis (PBC) data. The analysis reveals previously characterizing synchronized phase transitions in disease progression and identifying a parsimonious set of time-varying prognostic markers.

1 Introduction

Longitudinal studies, characterized by repeated observations of subjects over time, are a cornerstone of research in biomedicine (Fitzmaurice et al., 2012), economics (Baltagi, 2021), and social sciences. Classical tools for such data, such as linear mixed-effects models (LMMs) (Laird and Ware, 1982) and generalized estimating equations (GEE) (Liang and Zeger, 1986), have been foundational for decades. However, modern data acquisition technologies, from wearable devices to high-throughput biological assays, produce datasets that are not only high-dimensional ($p \gg n$) but also densely measured in time. This dense temporal structure places the analytical challenge at the intersection of classical longitudinal analysis and functional data analysis (FDA) (Ramsay and Silverman, 2005; Kokoszka and Reimherr, 2017).

A primary goal of FDA is to move beyond simple scalar covariate effects and model how associations vary smoothly as a function of time. The Time-Varying Coefficient Model (TVCM) is a key tool in this domain (Hastie and Tibshirani, 1993; Hoover et al., 1998; Fan and Zhang, 2008). By allowing covariate effects $\beta_j(t)$ to be flexible functions, TVCMs can capture complex, dynamic relationships. This is critical in applications like neuroimaging, where brain-behavior

*School of Statistics and Data Science, Capital University of Economics and Business, Beijing, China. Email: Skylinchern@cueb.edu.cn

†Corresponding author. Wisdom Lake Academy of Pharmacy, Xi'an Jiaotong-Liverpool University, Suzhou, China. Email: Mengfei.Ran@xjtlu.edu.cn

relationships are known to be non-static (Calhoun et al., 2014), or in understanding the time-varying impact of treatments and prognostic factors in progressive diseases.

The transition to functional models, however, introduces significant statistical and computational challenges. Estimating an entire function $\beta_j(t)$ for all p covariates is an ill-posed problem, often tackled by basis expansions (e.g., B-splines de Boor (2001)) or kernel smoothing (Wu et al., 1998). When p is large, this leads to an ultra-high-dimensional parametric problem, necessitating variable selection. While penalized methods like the Lasso (Tibshirani, 1996) are standard for scalar p , selecting an entire function $\beta_j(t)$ requires structured penalties. Methods have been proposed for functional variable selection, such as group-wise penalties on basis coefficients (Steinhardt et al., 2014; Fan et al., 2011; Fan and Lv, 2010; Jenatton et al., 2011).

However, several critical gaps remain in the literature. Standard ℓ_1 and group- ℓ_1 penalties (like the Group Lasso, Yuan and Lin (2006)) are known to produce biased estimates for large coefficients, thus failing to possess the oracle property (Fan and Li, 2001). This property, which ensures an estimator is as asymptotically efficient as if the true sparse model were known in advance, is crucial for accurate inference. This limitation can be overcome by using adaptive weights, as in the Adaptive Lasso (Zou, 2006) and its extensions (Wang and Leng, 2008), or by using non-convex penalties like SCAD (Fan and Li, 2001) or MCP (Zhang, 2010). Furthermore, standard functional models enforce smoothness (e.g., via $\int[\beta''(t)]^2 dt$). In many longitudinal applications, however, we are interested in abrupt changepoints, for instance, a sudden change in disease trajectory or symptom onset. The fused lasso (Tibshirani et al., 2005) and its variants (Rinaldo, 2009; Viallon et al., 2016) are designed for this, but are rarely integrated with high-dimensional functional variable selection. Finally, in many studies (e.g., clinical trials, neuroimaging), multiple correlated outcomes ($K > 1$) are collected. Analyzing each outcome separately is statistically inefficient. Joint modeling, or multi-task learning, can borrow strength across outcomes to improve estimation and selection accuracy (Obozinski et al., 2010; Caruana, 1997; Argyriou et al., 2008).

Unlike conventional baseline regression approaches that link baseline covariates to a single summary outcome (e.g., end-point value or subject-level average), AJL models the entire multi-outcome trajectory through time-varying effects $\beta_{jk}(t)$ and further detects shared changepoints in the population-level baseline curve $\alpha_k(t)$. This enables simultaneous characterization of when the overall trajectory exhibits structural transitions and which baseline features drive heterogeneous dynamics across correlated outcomes—capabilities that are unattainable via constant-effect regression or separate per-outcome analyses.

A unified framework that simultaneously (1) performs joint variable selection across multiple outcomes in a functional model, (2) detects abrupt changepoints in functional trajectories, and (3) possesses the oracle property for both selection and estimation, remains underdeveloped. This paper bridges these gaps by proposing a novel **Adaptive Joint Learning (AJL)** framework for high-dimensional functional longitudinal data. We model time-varying intercepts $\alpha_k(t)$ and coefficients $\beta_j(t)$ using B-spline basis expansions, transforming the functional problem into an ultra-high-dimensional parametric one. Our core contribution is a novel convex objective function that synthesizes three key ideas: an **Adaptive Group Lasso** on blocks of B-spline coefficients, to select entire functional covariates $\beta_j(t)$ that are relevant across all K outcomes; an adaptive fused lasso on the B-spline coefficients of the intercept functions $\alpha_k(t)$, to explicitly detect changepoints in their temporal dynamics; and the principle of adaptive weighting as a computationally tractable one-step Local Linear Approximation (LLA) (Zou and Li, 2008) of an ideal but intractable non-convex oracle problem. This innovative fusion of adaptive structured penalties is, to our knowledge, the first to provide a theoretically-backed oracle-performing estimator that jointly selects functional predictors and detects functional changepoints in a multi-task setting.

It is worth emphasizing that the theoretical integration of these components extends beyond a mere superposition of penalties. A primary theoretical hurdle lies in the structural interfer-

ence between the covariate selection space (governed by the group lasso) and the temporal segmentation space (governed by the fused lasso). In high-dimensional regimes, distinguishing between a smooth covariate effect and a structural intercept shift is theoretically precarious, as it requires rigorous incoherence conditions between the B-spline basis and the difference operator. Furthermore, the ‘Joint Learning’ aspect introduces a multi-objective optimization trade-off: attempting to enforce shared sparsity across heterogeneous outcomes (K) while locally identifying outcome-specific changepoints creates a conflict in regularization paths. Our theoretical analysis (Section 4) resolves these challenges by deriving uniform convergence rates that account for the simultaneous complexity of the discrete changepoint set and the continuous functional parameter space.

We develop a scalable multi-stage BCD-ADMM algorithm, provide a rigorous theoretical analysis with detailed proofs, and validate our method via extensive, redesigned simulation studies. Finally, we demonstrate the applicability of AJL by analyzing the classic Mayo Clinic Primary Biliary Cirrhosis (PBC) dataset. We jointly model the trajectories of three key liver function markers, identifying shared structural breakpoints in disease progression and revealing how the prognostic effects of baseline risk factors evolve dynamically over a decade of follow-up.

The remainder of this paper is organized as follows. Section 2 introduces the functional TVCM, the basis expansion, and the motivations for our penalized objective. Section 3 details the optimization procedure, including convergence and complexity analysis. Section 4 presents the core theoretical results, including the high-dimensional assumptions, non-asymptotic error bounds, and asymptotic oracle properties. Section 5 validates our method through extensive numerical studies. Section 6 provides a detailed application to PBC data analysis. Section 7 concludes. The Appendix contains proofs and discusses potential extensions.

2 Methodology

2.1 The Time-Varying Coefficient Model (TVCM)

We consider n subjects ($i = 1, \dots, n$) observed at possibly subject-specific and irregular visit times $t_{il} \in \mathcal{T}$, $l = 1, \dots, T_i$, with K scalar outcomes $y_{ilk} \in \mathbb{R}$, $k = 1, \dots, K$, recorded at each visit. For each subject i and outcome k , the collection $\{y_{ilk} : l = 1, \dots, T_i\}$ forms a longitudinal trajectory over the follow-up period.

While baseline covariates are prevalent in clinical studies, modern longitudinal designs (e.g., wearable sensors, intensive monitoring) often yield densely sampled predictor processes. To accommodate such complexity, we propose a general **Concurrent Varying-Coefficient Model (TVCM)** framework:

$$y_{ilk} = \alpha_k(t_{il}) + \sum_{j=1}^p x_{ij}(t_{il})\beta_{jk}(t_{il}) + \epsilon_{ilk}, \quad t_{il} \in \mathcal{T}, \quad (1)$$

where $\boldsymbol{\alpha}(t) = (\alpha_1(t), \dots, \alpha_K(t))^\top$ represents the K functional intercepts, and $\boldsymbol{\beta}_k(t) = (\beta_{1k}(t), \dots, \beta_{pk}(t))^\top$ denotes the vector of p time-varying functional coefficients for the k -th outcome. The errors ϵ_{ilk} are assumed to be independent with mean zero and finite variance.

This formulation encompasses two important statistical scenarios:

1. **Instantaneous Modulation:** The covariates $x_{ij}(t)$ vary continuously over time (e.g., concurrent EEG power predicting sleep depth), capturing dynamic dependencies.
2. **Baseline Prognosis:** The covariates are time-invariant baseline markers, i.e., $x_{ij}(t) \equiv x_{ij}$ (e.g., genetic risk scores or initial lab values), used to predict future disease trajectories.

In this article, we focus our numerical and empirical analysis primarily on the *Baseline Prognosis* case, as identifying early prognostic biomarkers remains a central challenge in precision

medicine. However, it is crucial to note that our proposed AJL framework and the associated B-spline design matrix construction apply seamlessly to the general time-varying case defined in (1) without algorithmic modification. Our goal is to jointly select the active functional predictors $\{\beta_{jk}(t)\}$ and identify structural change points in the intercept dynamics $\{\alpha_k(t)\}$.

2.2 Basis Expansion for Functional Data

Estimating the infinite-dimensional functions $\alpha_k(t)$ and $\beta_{jk}(t)$ directly is ill-posed. A standard and powerful approach is to approximate them using a linear combination of M basis functions (Ramsay and Silverman, 2005). Let $\phi(t) = (\phi_1(t), \dots, \phi_M(t))^\top$ be a vector of M basis functions defined over a set of knots on the domain \mathcal{T} .

Common choices for the basis include the Fourier basis and B-splines. The Fourier basis is an orthonormal basis on $[0, 1]$ given by $\phi_1(t) = 1$, $\phi_{2m}(t) = \sqrt{2} \cos(m\pi t)$, and $\phi_{2m+1}(t) = \sqrt{2} \sin(m\pi t)$. It is highly effective for smooth, periodic functions. However, our interest lies in modeling trajectories that may have abrupt, non-periodic changepoints. We therefore choose B-splines (de Boor, 2001) because they have local support (i.e., each $\phi_m(t)$ is non-zero only on a small interval). This local control is crucial for flexibly modeling non-periodic data and, as we will see, for representing abrupt changepoints, which a global basis like Fourier cannot do efficiently.

We approximate the unknown functions as:

$$\alpha_k(t) \approx \phi(t)^\top \mathbf{a}_k, \quad \text{where } \mathbf{a}_k = (a_{k1}, \dots, a_{kM})^\top \in \mathbb{R}^M \quad (2)$$

$$\beta_{jk}(t) \approx \phi(t)^\top \mathbf{b}_{jk}, \quad \text{where } \mathbf{b}_{jk} = (b_{jk1}, \dots, b_{jkM})^\top \in \mathbb{R}^M \quad (3)$$

The choice of M , the number of basis functions, is a crucial tuning parameter that controls a bias-variance trade-off. A small M may underfit (high bias), while a large M may overfit (high variance) and increases computational cost. In theory, M should grow slowly with N (e.g., $M \asymp N^{1/5}$) to achieve optimal non-parametric rates. In practice, M is often chosen to be large enough to capture the function's complexity and then fixed, with the subsequent regularization handling the overfitting.

Let $\mathbf{A} = [\mathbf{a}_1, \dots, \mathbf{a}_K] \in \mathbb{R}^{M \times K}$ be the coefficient matrix for all intercepts; and $\mathbf{B}_j = [\mathbf{b}_{j1}, \dots, \mathbf{b}_{jK}] \in \mathbb{R}^{M \times K}$ be the coefficient matrix for the j -th functional covariate across all K outcomes. Substituting these expansions into the model (1), we transform the functional model into an ultra-high-dimensional linear model. For the observation (i, t_{it}, k) :

$$y_{itk} \approx \phi(t_{it})^\top \mathbf{a}_k + \sum_{j=1}^p x_{ij} (\phi(t_{it})^\top \mathbf{b}_{jk}) + \epsilon_{itk} \quad (4)$$

This can be written in matrix form for all $N = \sum n_i$ observations. Let $\mathbf{Y} \in \mathbb{R}^{N \times K}$ be the stacked outcome matrix. Denote \mathbf{Z}_Φ be the $N \times M$ matrix where $[\mathbf{Z}_\Phi]_{il,m} = \phi_m(t_{il})$, and $\mathbf{X}_{\Phi,j}$ be the $N \times M$ matrix where $[\mathbf{X}_{\Phi,j}]_{il,m} = x_{ij} \phi_m(t_{il})$. The model becomes a high-dimensional multivariate regression on the $M(K + pK)$ coefficients:

$$\mathbf{Y} \approx \mathbf{Z}_\Phi \mathbf{A} + \sum_{j=1}^p \mathbf{X}_{\Phi,j} \mathbf{B}_j + \mathbf{E} \quad (5)$$

Our task is to estimate \mathbf{A} and the \mathbf{B}_j matrices under sparsity and changepoint constraints.

2.3 Advantages of the Functional Basis Parameterization

This transformation from an infinite-dimensional functional problem to an ultra-high-dimensional parametric one is not merely a convenience; it is a theoretically motivated strategy. First, the

local support of B-splines (Assumption 5) means the design matrix Φ is sparse, which generally improves the condition number and stability of the estimation problem compared to dense kernel matrices. Second, the local parameterization allows us to design penalties that target specific functional features. As we will see, applying a fused lasso to adjacent B-spline coefficients $|a_{k,m+1} - a_{k,m}|$ is a principled way to enforce piecewise-constant structure in $\alpha_k(t)$. This is only meaningful because B-spline basis functions $\phi_m(t)$ and $\phi_{m+1}(t)$ are neighbors in time. Third, the problem is naturally structured into p blocks $\{\mathbf{B}_j\}$, each of size $M \times K$. This perfectly aligns with our goal of selecting an entire function $\beta_j(t)$. Our penalty will be a sum of penalties on these blocks, $P(\mathbf{B}) = \sum_j P_j(\mathbf{B}_j)$, which is a classic decomposable regularizer (Negahban et al., 2012). Finally, this framework naturally handles irregular observation times t_{il} and missing data by simply evaluating the basis functions $\phi(t_{il})$ at the times that are observed.

2.4 A Penalized Objective for Functional Data

We jointly estimate the coefficient matrices \mathbf{A} and $\{\mathbf{B}_j\}_{j=1}^p$ by minimizing a penalized least-squares loss. The core innovation is to design penalties on the coefficients that enforce our desired functional properties. This is a crucial step that imbues the parametric model with functional characteristics.

Our first goal is functional variable selection: we want to identify which covariates j are irrelevant, i.e., $\beta_j(t) \equiv 0$ for all $t \in \mathcal{T}$ and all outcomes $k = 1, \dots, K$. In the B-spline framework, this is equivalent to selecting the entire coefficient matrix $\mathbf{B}_j = [\mathbf{b}_{j1}, \dots, \mathbf{b}_{jK}] \in \mathbb{R}^{M \times K}$ as a single group. A natural penalty to enforce this group-wise sparsity is the Frobenius (or $\ell_{2,1}$) norm on each block (Lounici et al., 2011):

$$P_g(\{\mathbf{B}_j\}) = \sum_{j=1}^p \|\mathbf{B}_j\|_F, \quad \text{where } \|\mathbf{B}_j\|_F = \left(\sum_{k=1}^K \sum_{m=1}^M b_{jkm}^2 \right)^{1/2} \quad (6)$$

This penalty is the empirical counterpart to penalizing the L^2 -norm of the functional coefficient block. To see this, note that $\sum_k \int \beta_{jk}(t)^2 dt = \sum_k \int \mathbf{b}_{jk}^\top \phi(t) \phi(t)^\top \mathbf{b}_{jk} dt = \sum_k \mathbf{b}_{jk}^\top \Sigma_\phi \mathbf{b}_{jk}$, where $\Sigma_\phi = \int \phi(t) \phi(t)^\top dt$. If the basis is orthonormal ($\Sigma_\phi = \mathbf{I}_M$), this simplifies to $\sum_k \|\mathbf{b}_{jk}\|_2^2 = \|\mathbf{B}_j\|_F^2$. While B-splines are not perfectly orthonormal, $\|\mathbf{B}_j\|_F$ remains a highly effective and computationally convenient proxy for the functional L^2 -norm. Applying this penalty encourages entire matrices \mathbf{B}_j to be set to exactly $\mathbf{0}$, thus selecting functional covariate \mathbf{x}_j out of the model.

Our second, equally important goal is to detect changepoints in the intercept functions $\alpha_k(t)$. Standard functional penalties (e.g., $\int [\alpha_k''(t)]^2 dt$) enforce smoothness and correspond to ℓ_2 penalties on coefficient differences (e.g., $\|\mathbf{D}_2 \mathbf{a}_k\|_2^2$, where \mathbf{D}_2 is a second-order difference operator). These penalties are excellent for estimating smooth curves but will blur and hide abrupt changepoints, which are often of primary clinical or economic interest (Safikhani and Shojaie, 2022).

To explicitly detect changepoints, we want to find an $\alpha_k(t)$ that is piecewise constant. Due to the local support property of B-splines, a piecewise-constant function $\alpha_k(t)$ corresponds to a coefficient vector \mathbf{a}_k that is itself piecewise constant. We can enforce this structure by applying the fused lasso (or total variation) penalty, which is an ℓ_1 penalty on the first-differences of the adjacent B-spline coefficients:

$$P_f(\mathbf{A}) = \sum_{k=1}^K \|\mathbf{D}_1 \mathbf{a}_k\|_1 = \sum_{k=1}^K \sum_{m=1}^{M-1} |a_{k,m+1} - a_{k,m}| \quad (7)$$

where \mathbf{D}_1 is the first-difference operator matrix. This penalty shrinks successive differences $(a_{k,m+1} - a_{k,m})$ towards zero. The result is an estimated vector $\hat{\mathbf{a}}_k$ that is sparse in its differences, i.e., piecewise constant. This, in turn, produces an estimated function $\hat{\alpha}_k(t) = \phi(t)^\top \hat{\mathbf{a}}_k$ that

is a (locally smoothed) piecewise-constant function. The locations m where $\hat{a}_{k,m+1} \neq \hat{a}_{k,m}$ correspond to the detected changepoints.

Combining these elements, our baseline (non-adaptive) joint functional model is the solution to:

$$\min_{\mathbf{A}, \{\mathbf{B}_j\}} \frac{1}{2N} \|\mathbf{Y} - \mathbf{Z}_\Phi \mathbf{A} - \sum_{j=1}^p \mathbf{X}_{\Phi,j} \mathbf{B}_j\|_F^2 + \lambda_g \sum_{j=1}^p \|\mathbf{B}_j\|_F + \lambda_f \sum_{k=1}^K \|\mathbf{D}_1 \mathbf{a}_k\|_1 \quad (8)$$

We have omitted the optional weight matrix \mathbf{W} for simplicity.

2.5 Theoretical Motivation for Adaptivity

The baseline model (8), while functional and structured, still suffers from the fundamental estimation bias inherent in ℓ_1 and Frobenius-norm penalties (Fan and Li, 2001; Zou, 2006). The constant shrinkage applied by λ_g and λ_f biases the estimates of non-zero coefficients towards zero, preventing the estimator from achieving the oracle property.

Our goal is to find an estimator that is as efficient as an oracle estimator, i.e., an unpenalized estimator that knows the true active set \mathcal{S} and the true changepoint locations $\{\mathcal{C}_k\}$ in advance. This property can be achieved by non-convex penalties (e.g., SCAD, MCP), but this leads to a difficult, non-convex optimization problem.

Instead, we follow the insight of Zou and Li (2008) and motivate our AJL framework as a computationally tractable, one-step Local Linear Approximation (LLA) to the ideal but intractable non-convex functional problem:

$$\min_{\mathbf{A}, \{\mathbf{B}_j\}} L_N(\mathbf{A}, \{\mathbf{B}_j\}) + \sum_{j=1}^p p_{\lambda_g}(\|\mathbf{B}_j\|_F) + \sum_{k=1}^K \sum_{m=1}^{M-1} p_{\lambda_f}(|a_{k,m+1} - a_{k,m}|). \quad (9)$$

where $p_\lambda(\cdot)$ is an oracle penalty like SCAD. The LLA of this problem is a weighted ℓ_1 -type problem, which can be solved in a 3-stage, convex-only procedure: (1) get initial consistent estimates $(\tilde{\mathbf{A}}, \tilde{\mathbf{B}})$ from (8), (2) compute data-driven weights, and (3) solve the final weighted convex problem.

2.6 The Generalized Adaptive Joint Learning (AJL) Objective

We propose a unified and generalized Adaptive Joint Learning (AJL) objective. Unlike traditional methods that treat variable selection and structural change detection as separate tasks, our framework formulates them as a joint convex optimization problem. This generalized formulation allows for the simultaneous discovery of (i) significant functional predictors, (ii) shared regime shifts in baseline processes, and (iii) dynamic structural changes in covariate effects. The estimator is defined as the global minimizer of:

$$\begin{aligned} Q(\theta) = & \frac{1}{2N} \left\| \mathbf{Y} - \mathbf{Z}_\Phi \mathbf{A} - \sum_{j=1}^p \mathbf{X}_{\Phi,j} \mathbf{B}_j \right\|_F^2 + \lambda_g \sum_{j=1}^p \hat{w}_{g,j} \|\mathbf{B}_j\|_F & \text{(Selection)} \\ & + \lambda_f^\alpha \sum_{k=1}^K \sum_{m=1}^{M-1} \hat{w}_{f,km}^\alpha |a_{k,m+1} - a_{k,m}| & \text{(Intercept Shifts)} \\ & + \lambda_f^\beta \sum_{j=1}^p \sum_{k=1}^K \sum_{m=1}^{M-1} \hat{w}_{f,jkm}^\beta |b_{jk,m+1} - b_{jk,m}| & \text{(Effect Dynamics)} \end{aligned} \quad (10)$$

This generalized formulation introduces three distinct regularization components:

1. Adaptive Group Lasso: Selects significant functional predictors by encouraging sparsity on the block norms $\|\mathbf{B}_j\|_F$.

2. Adaptive Intercept Fusion: Detects structural breaks in the baseline processes $\alpha_k(t)$.
3. Adaptive Slope Fusion: The term with λ_f^β enforces piecewise-constant dynamics in the covariate effects $\beta_{jk}(t)$. This allows the model to identify critical time points where the relationship between a predictor and the outcome undergoes a structural shift (e.g., a "regime change" in treatment efficacy).

Remark 1 (Implicit Robustness to Outliers). While the proposed objective function (10) employs a squared Frobenius norm loss, which is classically sensitive to outliers due to the quadratic penalization of residuals, our framework inherently mitigates this sensitivity through the structural properties of the estimator.

First, the local support property of the B-spline basis (Assumption 5) ensures that the influence of an outlier at time t is confined to a small subset of adjacent coefficients, preventing global distortion of the estimated functional trajectory $\hat{\beta}_j(t)$. Unlike global bases (e.g., Fourier) where an outlier affects the entire curve, B-splines localize the error.

Second, the strong regularization imposed by the adaptive group and fused penalties acts as a barrier against overfitting. Even if the L_2 loss encourages the model to chase an outlier, the penalty terms suppress the emergence of complex, high-amplitude structures that do not align with the shared sparsity patterns or piecewise-constant dynamics enforced by the oracle weights.

Consequently, the AJL estimator maintains practical robustness without the computational complexity of non-smooth robust loss functions (e.g., Huber loss), a property we empirically validate under heavy-tailed and contaminated error scenarios in Section 5.

The weights are the key to achieving the oracle property. They are based on the initial consistent estimates $(\tilde{\mathbf{A}}, \tilde{\mathbf{B}}_j)$ from Stage 1.

1. **Adaptive Group Lasso Weights.** For the j -th functional covariate:

$$\hat{w}_{g,j} = \frac{1}{\|\tilde{\mathbf{B}}_j\|_F^{\gamma_g} + \epsilon_g}, \quad (11)$$

where $\gamma_g > 0$ (typically 1 or 2) and ϵ_g is a small stability constant (e.g., $1/N$). This adaptive reweighting follows the adaptive group Lasso principle (Wang and Leng, 2008), acting as a data-driven switch to separate signal from noise.

- **Case 1: Noise Variable** ($j \in \mathcal{S}^c$) Here, the true function $\beta_j^*(t) \equiv 0$, so the true coefficient matrix $\mathbf{B}_j^* = \mathbf{0}$. By consistency of the initial estimator (Assumption 3), $\|\tilde{\mathbf{B}}_j\|_F \xrightarrow{p} 0$. As the denominator goes to zero (plus ϵ_g), the weight $\hat{w}_{g,j} \rightarrow \infty$. The penalty for this variable, $\lambda_g \hat{w}_{g,j} \|\mathbf{B}_j\|_F$, becomes infinitely large for any $\|\mathbf{B}_j\|_F > 0$. This aggressively and consistently forces the final estimate $\hat{\mathbf{B}}_j$ to be exactly $\mathbf{0}$.
- **Case 2: Signal Variable** ($j \in \mathcal{S}$) Here, $\|\beta_j^*(t)\|_{L^2} = c_j > 0$, so $\|\mathbf{B}_j^*\|_F = c'_j > 0$. By consistency (Assumption 3), $\|\tilde{\mathbf{B}}_j\|_F \xrightarrow{p} c'_j > 0$. The weight $\hat{w}_{g,j} \rightarrow 1/(c_j^{\gamma_g} + \epsilon_g)$, which is a small, finite constant. The penalty for this variable is $\lambda_g \cdot (\text{const}) \cdot \|\mathbf{B}_j\|_F$. Since $\lambda_g \rightarrow 0$ is required for oracle property (Assumption 6), the penalty for true signals vanishes asymptotically.

This mechanism achieves both sparsity (by penalizing noise infinitely) and unbiasedness (by not penalizing signals).

2. **Adaptive Fused Lasso Weights.** For the m -th difference of the k -th intercept:

$$\hat{w}_{f,km} = \frac{1}{|\tilde{a}_{k,m+1} - \tilde{a}_{k,m}|^{\gamma_f} + \epsilon_f}, \quad (12)$$

This weight applies the exact same logic as above. If there is no true changepoint at m , then $\tilde{a}_{k,m+1} \approx \tilde{a}_{k,m}$, the denominator is near zero, and $\hat{w}_{f,km} \rightarrow \infty$, forcing $\hat{a}_{k,m+1} = \hat{a}_{k,m}$. If there *is* a true changepoint, the difference is non-zero, the weight is a finite constant, and the penalty vanishes, allowing the changepoint to be estimated without bias.

3. **Adaptive Slope Fusion Weights.** Analogous to the intercept term, we construct adaptive weights for the covariate coefficients to distinguish between smooth evolution and structural breaks. For the m -th difference of the j -th predictor's effect on outcome k :

$$\hat{w}_{f,jkm}^\beta = \frac{1}{|\tilde{b}_{jk,m+1} - \tilde{b}_{jk,m}|^{\gamma_s} + \epsilon_s} \quad (13)$$

These weights ensure that in the Refinement Phase, the penalty selectively enforces smoothness only where the initial estimates suggest no structural change, asymptotically reducing bias at true changepoints.

Remark 2 (Hierarchical Regularization Strategy and Computational Strategy). While the generalized objective (10) offers a holistic solution, simultaneously optimizing for selection and slope-segmentation in the ultra-high-dimensional regime ($p \gg n$) presents computational challenges and potential identification issues due to the interaction between the group-sparsity and fusion penalties.

To address this, we adopt a Hierarchical Regularization Strategy motivated by the principle of Sure Screening (Fan and Lv, 2008).

Screening Phase (Focus of this paper): We set $\lambda_f^\beta = 0$ (or sufficiently small) to prioritize the consistent recovery of the active support set \mathcal{S} via the Adaptive Group Lasso, while simultaneously detecting major baseline shifts via λ_f^α . This ensures that the dimensionality is effectively reduced from p to $s = |\mathcal{S}| \ll n$.

Refinement Phase: Conditional on the selected support \mathcal{S} , one can subsequently activate the slope fusion penalty ($\lambda_f^\beta > 0$) to refine the structural dynamics of the non-zero effects.

Our theoretical analysis in Section 4 demonstrates that the Screening Phase achieves the Oracle Property for variable selection. This implies that the separation of stages does not compromise the asymptotic validity of the estimator, but rather provides a numerically robust path to the global oracle solution. Consequently, our simulation studies and algorithm primarily focus on verifying the crucial Screening Phase.

While the objective in (10) is convex, solving it for ultra-high-dimensional p with simultaneous Group and Fused penalties on B_j can be computationally intensive. In practice, we often adopt a hierarchical strategy: we first set $\lambda_f^\beta = 0$ to identify the active support set \mathcal{S} via the Adaptive Group Lasso. Subsequently, we solve the full objective restricted to $j \in \mathcal{S}$ to refine the estimation of temporal dynamics. This two-stage procedure consistently recovers the oracle structure under the assumption that signal strength satisfies the "beta-min" condition, effectively reducing the computational complexity from $O(p)$ to $O(|\mathcal{S}|)$ for the fusion step.

3 Optimization Algorithm

The optimization of the AJL objective (10) follows the 3-stage procedure detailed in Algorithm 1. This is necessary because the weights \hat{w} in Stage 3 depend on the initial estimates $(\tilde{\mathbf{A}}, \tilde{\mathbf{B}})$ from Stage 1. The core solver for both Stage 1 and Stage 3 is a Block Coordinate Descent (BCD) algorithm (Algorithm 2), which iterates between optimizing \mathbf{A} and the set of $\{\mathbf{B}_j\}$. Each of these subproblems is convex and solved to high precision using the Alternating Direction Method of Multipliers (ADMM) (Boyd et al., 2011).

3.1 Convergence and Complexity Analysis

The BCD algorithm in Algorithm 2 is guaranteed to converge to a stationary point.

Proposition 1 (Convergence). *Let $Q(\mathbf{A}, \{\mathbf{B}_j\})$ be the (adaptive) objective function in (10). The objective function value $Q(\widehat{\mathbf{A}}^{(s)}, \{\widehat{\mathbf{B}}_j^{(s)}\})$ is monotonically decreasing in s and converges to a stationary point (a global minimum, as Q is convex).*

Proof. The objective Q is the sum of a smooth, convex loss function and two separable, convex, non-smooth penalties. The BCD update for each block (\mathbf{A} and each \mathbf{B}_j) exactly minimizes the objective with respect to that block, holding others fixed. This is a standard BCD procedure, and its convergence to a global minimum is a classic result in convex optimization. \square

Let $N_{\text{total}} = N \times K$ be the total number of observations. Let d_j be the complexity of solving the group lasso subproblem for \mathbf{B}_j (which is $M \times K$), and d_k be the complexity for the fused lasso subproblem for \mathbf{a}_k (which is $M \times 1$). A single sweep (iteration s) of Algorithm 2 has a complexity of $O(\sum_{j=1}^p (NMK + d_j) + \sum_{k=1}^K (NMK + d_k))$. The group lasso subproblem (proximal gradient) is efficient, $d_j \approx O(NMK)$. The fused lasso subproblem is a 1D Total Variation problem, which can be solved very efficiently, $d_k \approx O(M)$ using dynamic programming or $O(M \cdot I_{\text{ADMM}})$ via ADMM. Thus, the total complexity per sweep is dominated by the residual computations and is roughly $O(NMKp)$.

Algorithm 1 The 3-Stage AJL Algorithm

- 1: **Input:** Data $(\mathbf{Y}, \mathbf{X}, \mathbf{t})$, Basis $\phi(t)$, initial tuning $\lambda_g^{(0)}, \lambda_f^{(0)}$, final tuning λ_g, λ_f .
 - 2: Construct design matrices $\mathbf{Z}_\Phi, \mathbf{X}_\Phi$ from $\mathbf{X}, \mathbf{t}, \phi(t)$.
 - 3: **Stage 1: Initial Estimation**
 - 4: Obtain initial consistent coefficient estimates $(\tilde{\mathbf{A}}, \{\tilde{\mathbf{B}}_j\})$ by solving the *non-adaptive* problem:
 - 5: $(\tilde{\mathbf{A}}, \tilde{\mathbf{B}}_j) \leftarrow \arg \min_{\mathbf{A}, \mathbf{B}_j} \frac{1}{2N} \|\mathbf{Y} - \mathbf{Z}_\Phi \mathbf{A} - \sum_{j=1}^p \mathbf{X}_{\Phi, j} \mathbf{B}_j\|_F^2 + \lambda_g^{(0)} \sum_j \|\mathbf{B}_j\|_F + \lambda_f^{(0)} \sum_k \|\mathbf{D}_1 \mathbf{a}_k\|_1$
 - 6: \triangleright This is solved using the BCD-ADMM procedure (Algorithm 2).
 - 7: **Stage 2: Weight Calculation**
 - 8: For $j = 1, \dots, p$: $\hat{w}_{g,j} \leftarrow (\|\tilde{\mathbf{B}}_j\|_F^{\gamma_g} + \epsilon_g)^{-1}$
 - 9: For $k = 1, \dots, K$, $m = 1, \dots, M-1$: $\hat{w}_{f,km} \leftarrow (|\tilde{a}_{k,m+1} - \tilde{a}_{k,m}|^{\gamma_f} + \epsilon_f)^{-1}$
 - 10: **Stage 3: Adaptive Estimation**
 - 11: Obtain the final adaptive coefficient estimates $(\widehat{\mathbf{A}}, \{\widehat{\mathbf{B}}_j\})$ by solving (10):
 - 12: \triangleright This is also solved using BCD-ADMM (Algorithm 2).
 - 13: **Output:** Final functional estimates $\widehat{\alpha}_k(t) = \phi(t)^\top \widehat{\mathbf{a}}_k$, $\widehat{\beta}_{jk}(t) = \phi(t)^\top \widehat{\mathbf{b}}_{jk}$.
-

The core solver for both Stage 1 and Stage 3 is a Block Coordinate Descent (BCD) algorithm, which iterates between optimizing \mathbf{A} and the set of $\{\mathbf{B}_j\}$. Each of these subproblems is still complex and is solved using the Alternating Direction Method of Multipliers (ADMM) (Boyd et al., 2011).

Directly minimizing the fully generalized objective (10) involves coupled non-smooth penalties on B_j . To ensure computational scalability in ultra-high dimensions, we adopt a hierarchical optimization strategy. Algorithm 2 details the solver for the primary phase, where we focus on simultaneous variable selection (Group Lasso) and intercept segmentation (Fused Lasso), effectively setting $\lambda_f^\beta = 0$ during the screening process. Refined slope segmentation can be performed as a post-selection step on the active set \mathcal{S} .

Algorithm 2 BCD-ADMM for the Reduced AJL Problem (Stages 1 and 3 of Algorithm 1, Intercept-Fusion Focus)

```

1: Input:  $\mathbf{Y}, \mathbf{Z}_\Phi, \{\mathbf{X}_{\Phi,j}\}, \lambda_g, \lambda_f$ , weights  $\hat{\mathbf{w}}_g, \hat{\mathbf{w}}_f$ .
2: Initialize:  $\hat{\mathbf{A}}^{(0)}, \{\hat{\mathbf{B}}_j^{(0)}\}$ . Let  $s = 0$ .
3: repeat
4:    $s \leftarrow s + 1$ .
5:   Update  $\mathbf{B}$  (Adaptive Group Lasso)
6:   Compute partial residual  $\mathbf{R} = \mathbf{Y} - \mathbf{Z}_\Phi \hat{\mathbf{A}}^{(s-1)}$ .
7:   For each  $j = 1, \dots, p$ :
8:      $\hat{\mathbf{B}}_j^{(s)} \leftarrow \arg \min_{\mathbf{B}_j} \frac{1}{2N} \|\mathbf{R} - \mathbf{X}_{\Phi,j} \mathbf{B}_j\|_F^2 + \lambda_g \hat{w}_{g,j} \|\mathbf{B}_j\|_F$ 
9:      $\triangleright$  This is a standard Group Lasso problem, solved via ADMM/proximal gradient.
10:  EndFor
11:  Update  $\mathbf{A}$  (Adaptive Fused Lasso)
12:  Compute partial residual  $\mathbf{E} = \mathbf{Y} - \sum_{j=1}^p \mathbf{X}_{\Phi,j} \hat{\mathbf{B}}_j^{(s)}$ .
13:  For each outcome  $k = 1, \dots, K$  in parallel:
14:     $\hat{\mathbf{a}}_k^{(s)} \leftarrow \arg \min_{\mathbf{a}_k} \frac{1}{2N} \|\mathbf{E}_{\cdot k} - \mathbf{Z}_\Phi \mathbf{a}_k\|_2^2 + \lambda_f \sum_{m=1}^{M-1} \hat{w}_{f,km} |a_{k,m+1} - a_{k,m}|$ 
15:     $\triangleright$  This is a weighted Fused Lasso (1D-TV) problem, solved efficiently via ADMM or
       dynamic programming.
16:  EndFor
17: until convergence of  $(\hat{\mathbf{A}}^{(s)}, \{\hat{\mathbf{B}}_j^{(s)}\})$ .
18: Return:  $\hat{\mathbf{A}} = \hat{\mathbf{A}}^{(s)}, \{\hat{\mathbf{B}}_j\} = \{\hat{\mathbf{B}}_j^{(s)}\}$ .

```

4 Theoretical Analysis

We establish the oracle properties of our functional estimator $\hat{\beta}(t)$. The theory is developed for the B-spline coefficient estimators $(\hat{\mathbf{A}}, \hat{\mathbf{B}})$ under an asymptotic regime where the number of basis functions $M = M_N$ may grow with N , and $p = p_N$ may grow as well.

Unlike prior works that treat structural discovery and variable selection in isolation, our theoretical analysis establishes the oracle properties for the comprehensive Generalized AJL objective (10), fully incorporating the slope-fusion regularization component. Leveraging the block-decomposability of B-spline coefficients and the structural isomorphism between intercept and slope difference penalties, we derive the consistency and asymptotic normality for the full estimator. Furthermore, we explicitly provide the theoretical justification for the Hierarchical Regularization Strategy (Remark 2). By establishing the *Sure Screening Property* of the initial stage, we guarantee that the computationally efficient screening phase consistently recovers the true active set, thereby validating the asymptotic optimality of the sequential refinement procedure.

4.1 Assumptions

We require a set of standard, rigorous assumptions for high-dimensional functional regression. Let $\mathcal{S} = \{j : \|\beta_j^*\|_{L^2} > 0\}$ be the true active set of functional covariates ($s = |\mathcal{S}|$); and $\mathcal{C}_k = \{m : a_{k,m+1}^* \neq a_{k,m}^*\}$ be the changepoints in the B-spline coefficients for $\alpha_k(t)$.

Assumption 1 (Error Distribution). *The error vectors $\epsilon_i = (\epsilon_{i,t_{i1},1}, \dots, \epsilon_{i,t_{in_i},K})^\top$ for each subject i are independent, zero-mean, sub-Gaussian random vectors. Their covariance $\Sigma_{\epsilon,i} = \mathbb{E}[\epsilon_i \epsilon_i^\top]$ is a block matrix that allows for arbitrary correlation within the subject (i.e., across time and outcomes). This clustered sub-Gaussian assumption is more realistic than i.i.d. errors.*

Assumption 2 (Approximation Error). *The true functions $\alpha_k^*(t)$ and $\beta_{jk}^*(t)$ are in a Sobolev space of order $d > 1$. The B-spline basis (with M functions) is chosen such that the approximation error is well-controlled: $\max_k \|\alpha_k^* - \phi^\top \mathbf{a}_k^*\|_\infty = O_p(M^{-d})$ and $\max_{j,k} \|\beta_{jk}^* - \phi^\top \mathbf{b}_{jk}^*\|_\infty = O_p(M^{-d})$.*

Assumption 3 (Initial Estimator Consistency). *The initial B-spline coefficient estimators $(\tilde{\mathbf{A}}, \{\tilde{\mathbf{B}}_j\})$ are consistent. Specifically, they converge to the true coefficients $(\mathbf{A}^*, \{\mathbf{B}_j^*\})$ at a sufficient rate, e.g., $\max_j \|\tilde{\mathbf{B}}_j - \mathbf{B}_j^*\|_F = O_p(\sqrt{M \log(p)/N})$.*

Assumption 4 (Design Matrix Regularity). *The design matrix Φ constructed from the B-spline bases satisfies the following regularity conditions on the high-dimensional coefficient space:*

1. **Restricted Strong Convexity (RSC):** For any Δ in the restricted cone $\mathbb{C} = \{\Delta : \mathcal{R}(\theta^* + \Delta) \leq \mathcal{R}(\theta^*) + \text{tol}\}$ induced by the adaptive penalties, the empirical loss satisfies a block-wise Restricted Strong Convexity (RSC) condition (Negahban et al., 2012):

$$L_N(\theta^* + \Delta) - L_N(\theta^*) - \langle \nabla L_N(\theta^*), \Delta \rangle \geq \kappa \|\Delta\|_2^2 - \tau \Psi^2(\Delta), \quad (14)$$

where $\kappa > 0$ is the curvature constant and $\Psi(\Delta)$ is the regularization function (e.g., the weighted ℓ_1 -norm).

2. **Block-Irrepresentable Condition (Block-IRC):** Let $\mathbf{H} = \frac{1}{N} \Phi^\top \Phi$ be the empirical covariance matrix. There exists an incoherence parameter $\eta \in (0, 1]$ such that for the true active set \mathcal{S} and any inactive block $j \notin \mathcal{S}$,

$$\|\mathbf{H}_{j\mathcal{S}}(\mathbf{H}_{\mathcal{S}\mathcal{S}})^{-1}\|_{\infty, \text{block}} \leq 1 - \eta. \quad (15)$$

Remark 3 (Adaptation and Relaxation). We explicitly note that strict application of these conditions requires adaptation in our functional setting. First, regarding **RSC**: Although B-spline bases exhibit intrinsic local correlations, the *Riesz basis property* (Assumption 5) ensures that the eigenvalues of the Gram matrix are bounded, implying that curvature in the coefficient space (ℓ_2 -norm) effectively translates to identifiability in the functional space (L^2 -norm). Second, regarding **Block-IRC**: While standard Lasso consistency requires the strict incoherence condition above, our *Adaptive* framework relaxes this requirement. As demonstrated in the proof of Theorem 2, the diverging adaptive weights for noise variables ($\hat{w}_{g,j} \rightarrow \infty$) allow the estimator to achieve consistent selection even when the strict Block-IRC is violated (i.e., in the presence of higher collinearity), aligning with our simulation results in Scenario 5.

Assumption 5 (Basis Functions). *The basis functions are uniformly bounded, $\sup_{t \in \mathcal{T}} \|\phi(t)\|_\infty \leq C_\phi$ for some constant $C_\phi < \infty$. The matrix $\Sigma_\phi = \mathbb{E}[\phi(t)\phi(t)^\top]$ is positive definite with eigenvalues bounded in $[\lambda_{\min}, \lambda_{\max}]$, where $0 < \lambda_{\min} \leq \lambda_{\max} < \infty$. This is a standard condition satisfied by B-splines. In the general case of time-varying covariates (as defined in Section 2.1), we further assume that the expected covariance operator of the predictor processes $x(t)$ is non-degenerate with respect to the B-spline basis. This ensures that the time-varying design matrix X_Φ inherits the restricted eigenvalue properties required for the RSC condition (Assumption 4).*

Assumption 6 (Tuning and Adaptive Weights). *Let $\gamma_g, \gamma_\alpha, \gamma_\beta > 1$ be pre-specified constants. We define the adaptive weights as:*

$$w_{g,j} = \{\|\tilde{\mathbf{B}}_j\|_F + \tau_N\}^{-\gamma_g}, \quad w_{f,k,m}^\alpha = \{|\Delta \tilde{a}_{k,m}| + \tau_N\}^{-\gamma_\alpha}, \quad w_{f,j,k,m}^\beta = \{|\Delta \tilde{b}_{jk,m}| + \tau_N\}^{-\gamma_\beta},$$

where $\tau_N \asymp N^{-1/2}$ is a ridge parameter to prevent division by zero.

Suppose the initial estimator $(\tilde{\mathbf{A}}, \tilde{\mathbf{B}})$ satisfies the standard consistency rates such that for the true active set \mathcal{S} , intercept changepoints \mathcal{C}^α , and slope changepoints \mathcal{C}^β :

- **Selection Strength:** $\min_{j \in \mathcal{S}} \|\tilde{\mathbf{B}}_j\|_F \geq c_B N^{-\kappa}$ for some $\kappa \in [0, 1/2)$;
- **Jump Detection:** $\min_{(k,m) \in \mathcal{C}^\alpha} |\Delta \tilde{a}_{k,m}| \geq c_\alpha N^{-\kappa}$ and $\min_{(j,k,m) \in \mathcal{C}^\beta} |\Delta \tilde{b}_{jk,m}| \geq c_\beta N^{-\kappa}$.

Let the tuning parameters obey the following rates ensuring correct selection and structural discovery:

$$\lambda_g \asymp c_g \sqrt{\frac{\log p}{N}}, \quad \lambda_f^\alpha \asymp c_\alpha \sqrt{\frac{\log(MK)}{N}}, \quad \lambda_f^\beta \asymp c_\beta \sqrt{\frac{\log(pMK)}{N}}.$$

Assume that as $N \rightarrow \infty$, all $\lambda \rightarrow 0$ and $\sqrt{N}\lambda \rightarrow \infty$. Furthermore, the adaptive weights satisfy the Oracle Separation Conditions:

$$\begin{aligned} \max_{j \in \mathcal{S}} \sqrt{N} \lambda_g w_{g,j} &= o_p(1), & \min_{j \notin \mathcal{S}} \sqrt{N} \lambda_g w_{g,j} &\rightarrow \infty; \\ \max_{(k,m) \in \mathcal{C}^\alpha} \sqrt{N} \lambda_f^\alpha w_{f,k,m}^\alpha &= o_p(1), & \min_{(k,m) \notin \mathcal{C}^\alpha} \sqrt{N} \lambda_f^\alpha w_{f,k,m}^\alpha &\rightarrow \infty; \\ \max_{(j,k,m) \in \mathcal{C}^\beta} \sqrt{N} \lambda_f^\beta w_{f,j,k,m}^\beta &= o_p(1), & \min_{(j,k,m) \notin \mathcal{C}^\beta} \sqrt{N} \lambda_f^\beta w_{f,j,k,m}^\beta &\rightarrow \infty. \end{aligned}$$

Assumption 7 (Undersmoothing for Inference). *In addition to the conditions in Assumption 6, we require the number of basis functions M_N to satisfy $N M_N^{-2d} \rightarrow 0$ as $N \rightarrow \infty$. This implies $M_N \gg N^{1/2d}$. Justification: This condition ensures that the squared approximation bias decays faster than the parametric rate N^{-1} , rendering the bias asymptotically negligible compared to the variance for valid inference.*

In essence, Assumptions 1-7 ensure that: (i) the errors are clustered sub-Gaussian (Assumption 1); (ii) the functional approximation bias is controlled (Assumption 2); (iii) the initial estimator is consistent (Assumption 3); (iv) the functional design satisfies a restricted strong convexity condition (Assumption 4) together with well-behaved basis functions (Assumption 5); and (v) the tuning parameters and adaptive weights lie in an appropriate high-dimensional regime (Assumption 6); (vi) Assumption 7 ensures that the squared approximation bias decays faster than the parametric rate N^{-1} , rendering the bias asymptotically negligible compared to the variance for valid inference.

4.2 Non-Asymptotic Analysis

Let $\boldsymbol{\theta} = \text{vec}(\mathbf{A}, \mathbf{B}_1, \dots, \mathbf{B}_p)$ be the vector of all coefficients. Following the modern framework for high-dimensional M-estimators (Bühlmann and van de Geer, 2011; Negahban et al., 2012), we first establish non-asymptotic error bounds.

Lemma 1 (Basic Inequality). *Let $\hat{\theta}$ be the solution to (10). For any $\boldsymbol{\theta}^*$, the following inequality holds:*

$$L_N(\hat{\theta}) - L_N(\boldsymbol{\theta}^*) + P_{\text{ada}}(\hat{\theta}) - P_{\text{ada}}(\boldsymbol{\theta}^*) \leq 0 \quad (16)$$

By convexity of L_N and properties of the decomposable penalty P_{ada} , this leads to a bound on the error $\Delta = \hat{\theta} - \boldsymbol{\theta}^*$ based on the gradient $\nabla L_N(\boldsymbol{\theta}^*)$ and the penalty structure.

Theorem 1 (Estimation Error Rate of Generalized AJL). *Under Assumptions 1-6, and assuming the tuning parameters satisfy the rates specified in Assumption 6 (i.e., dominating the stochastic noise levels), the generalized AJL estimator $\hat{\theta} = (\hat{\mathbf{A}}, \hat{\mathbf{B}})$ satisfies the following non-asymptotic error bounds with probability approaching one:*

$$\begin{aligned} \|\hat{\mathbf{A}} - \mathbf{A}^*\|_F^2 &\lesssim |\mathcal{C}^\alpha|(\lambda_f^\alpha)^2, \\ \sum_{j=1}^p \|\hat{\mathbf{B}}_j - \mathbf{B}_j^*\|_F^2 &\lesssim \underbrace{s \lambda_g^2}_{\text{Sparsity Cost}} + \underbrace{|\mathcal{C}^\beta|(\lambda_f^\beta)^2}_{\text{Dynamic Cost}}. \end{aligned}$$

In a unified form, the total estimation error is bounded by:

$$\|\hat{\theta} - \theta^*\|_2^2 \lesssim |\mathcal{C}^\alpha|(\lambda_f^\alpha)^2 + s\lambda_g^2 + |\mathcal{C}^\beta|(\lambda_f^\beta)^2.$$

These bounds explicitly characterize the trade-off between model complexity and estimation precision. Specifically, the error is governed by the **structural sparsity** of the true model: the number of active predictors (s), the number of baseline regime shifts ($|\mathcal{C}^\alpha|$), and the number of dynamic structural changes in covariate effects ($|\mathcal{C}^\beta|$).

Theorem 2 (Consistent Support Recovery & Structural Localization). *Suppose Assumptions 1-6 hold. Let the minimum signal strength satisfy the Beta-min condition:*

$$\begin{aligned} \min_{j \in \mathcal{S}} \|\mathbf{B}_j^*\|_F &\geq c_B \sqrt{\frac{\log p}{N}}, \\ \min_{(k,m) \in \mathcal{C}^\alpha} |\Delta a_{k,m}^*| &\geq c_\alpha \sqrt{\frac{\log(MK)}{N}}, \\ \min_{(j,k,m) \in \mathcal{C}^\beta} |\Delta b_{jk,m}^*| &\geq c_\beta \sqrt{\frac{\log(pMK)}{N}}. \end{aligned}$$

Under the Block-Irrepresentable Condition (Block-IRC) on the design matrix, the Generalized AJL estimator satisfies the following properties with probability approaching one (w.p.a.1) as $N \rightarrow \infty$:

1. **Model Selection Consistency:** The active set of functional predictors is correctly recovered:

$$\text{supp}(\hat{\mathbf{B}}) = \mathcal{S}.$$

2. **Baseline Regime Identification:** The locations of structural breaks in the baseline intercept functions are consistently estimated:

$$\hat{\mathcal{C}}_k^\alpha = \mathcal{C}_k^{\alpha,*} \quad \forall k = 1, \dots, K.$$

3. **Dynamic Effect Segmentation:** For all selected predictors $j \in \mathcal{S}$, the internal structural changes in their time-varying effects are correctly localized:

$$\hat{\mathcal{C}}_{jk}^\beta = \mathcal{C}_{jk}^{\beta,*} \quad \forall j \in \mathcal{S}, k = 1, \dots, K.$$

This theorem implies that the AJL framework achieves **full structural oracle properties**. It not only distinguishes relevant variables from noise but also disentangles smooth evolution from abrupt regime shifts within the identified signal, providing a complete structural roadmap of the high-dimensional longitudinal process.

Proposition 2 (Validity of Hierarchical Screening). *Consider the **Screening Phase** of the proposed algorithm, where the estimator $\hat{\theta}^{\text{screen}} = (\hat{\mathbf{A}}, \hat{\mathbf{B}})$ is obtained by minimizing the objective function (10) with the slope-fusion constraint forced to zero (i.e., $\lambda_f^\beta = 0$), while λ_g and λ_f^α satisfy the rates in Assumption 6. Let $\hat{\mathcal{S}}_{\text{screen}} = \{j : \|\hat{\mathbf{B}}_j\|_F > 0\}$ denote the active set selected in this phase. Under the Beta-min condition (Assumption 6) and the Block-Irrepresentable Condition, the screening procedure satisfies the **Sure Screening Property**:*

$$\mathbb{P}(\mathcal{S}^* \subseteq \hat{\mathcal{S}}_{\text{screen}}) \rightarrow 1 \quad \text{as } N \rightarrow \infty.$$

Remark 4. Proposition 2 provides the theoretical justification for our Hierarchical Regularization Strategy. It guarantees that, with probability approaching one, the initial screening step retains all truly relevant predictors. Consequently, the subsequent refinement step (where $\lambda_f^\beta > 0$ is activated) operates within a subspace that contains the true model, ensuring that the final structural discovery is asymptotically unbiased.

The proofs of Lemma 1, Theorems 1 and 2 are non-trivial and build on extensions of the general frameworks in Negahban et al. (2012) and Bühlmann and van de Geer (2011) to our adaptive fused-group structure; detailed arguments are provided in Appendix A.

4.3 Asymptotic Oracle Property

We now show that under the specific high-dimensional rates from Assumption 6, our estimator achieves the oracle property.

Theorem 3 (Asymptotic Selection Consistency). *Let $(\hat{\mathbf{A}}, \{\hat{\mathbf{B}}_j\})$ be the solution to the AJL problem (10). Under Assumptions 1-6, the estimator is selection-consistent:*

1. $\Pr(\{j : \|\hat{\mathbf{B}}_j\|_F > 0\} = \mathcal{S}) \rightarrow 1$ as $N \rightarrow \infty$.
2. $\Pr(\{m : \hat{a}_{k,m+1} \neq \hat{a}_{k,m}\} = \mathcal{C}_k, \forall k) \rightarrow 1$ as $N \rightarrow \infty$.

Theorem 4 (Asymptotic Normality and Valid Inference). *Suppose Assumptions A1-A6 hold, and additionally, the **Undersmoothing Condition** (Assumption 7) is satisfied (i.e., $NM_N^{-2d} \rightarrow 0$ where d is the spline smoothness order). Let $\mathcal{A} = \mathcal{S} \cup \mathcal{C}^\alpha \cup \mathcal{C}^\beta$ denote the **Global Oracle Set**, comprising the true active predictors, baseline changepoints, and slope dynamics. Let $\hat{\boldsymbol{\theta}}_{\mathcal{A}}$ be the vector of estimated coefficients restricted to this set. Then, the estimator satisfies:*

1. **Oracle Distribution of Coefficients:** The penalized estimator behaves asymptotically as the unpenalized Oracle estimator on the true support:

$$\sqrt{N} \boldsymbol{\Sigma}_{\mathcal{A}}^{-1/2} (\hat{\boldsymbol{\theta}}_{\mathcal{A}} - \boldsymbol{\theta}_{\mathcal{A}}^*) \xrightarrow{d} \mathcal{N}(\mathbf{0}, \mathbf{I}), \quad (17)$$

where $\boldsymbol{\theta}_{\mathcal{A}}^*$ is the projection of the true functions onto the B-spline space, and $\boldsymbol{\Sigma}_{\mathcal{A}} = \sigma_\epsilon^2 (\mathbb{E}[\mathbf{Z}_{\mathcal{A}}^\top \mathbf{Z}_{\mathcal{A}}])^{-1}$ is the asymptotic covariance matrix of the Oracle sub-model.

2. **Pointwise Functional Inference:** For any active predictor $j \in \mathcal{S}$ and any time point $t \in \mathcal{T}$ that is not a changepoint, the estimated time-varying coefficient $\hat{\beta}_j(t)$ follows:

$$\frac{\hat{\beta}_j(t) - \beta_j^*(t)}{\hat{\sigma}_j(t)} \xrightarrow{d} \mathcal{N}(0, 1), \quad (18)$$

where $\beta_j^*(t)$ is the true functional curve (not just the spline approximation). The standard error $\hat{\sigma}_j(t)$ is consistently estimated via the plug-in estimator:

$$\hat{\sigma}_j^2(t) = \boldsymbol{\phi}(t)^\top [\widehat{\text{Cov}}(\hat{\boldsymbol{\theta}}_{\mathcal{A}})]_{jj} \boldsymbol{\phi}(t).$$

The significance of (18) lies in the validity of post-selection inference. The Undersmoothing Condition ensures that the squared approximation bias is asymptotically negligible compared to the variance ($\text{bias}^2 \ll \text{var}$). Consequently, we can construct valid $(1 - \alpha)$ confidence intervals for the dynamic effects as $\hat{\beta}_j(t) \pm z_{\alpha/2} \hat{\sigma}_j(t)$, treating the selected structure as fixed.

Remark 5 (Role of Undersmoothing). A critical distinction must be made between estimating the "best projection" of the function and the function itself. The asymptotic normality in equation (17) applies to the coefficients $\boldsymbol{\theta}^*$. However, for the functional estimator $\hat{\beta}(t)$, the total error decomposes into:

$$\hat{\beta}(t) - \beta^*(t) = \underbrace{\boldsymbol{\phi}(t)^\top (\hat{\boldsymbol{\theta}} - \boldsymbol{\theta}^*)}_{\text{Stochastic Term}} + \underbrace{(\boldsymbol{\phi}(t)^\top \boldsymbol{\theta}^* - \beta^*(t))}_{\text{Approximation Bias}}$$

Standard estimation rates (e.g., for optimal MSE) typically balance the squared bias and variance, leaving a non-vanishing bias in the limiting distribution. By enforcing the undersmoothing condition (Assumption 7, $NM^{-2d} \rightarrow 0$), we ensure that the bias term is $o_p(N^{-1/2})$. Consequently, the asymptotic distribution is dominated solely by the stochastic term, validating the construction of confidence intervals centered at $\hat{\beta}(t)$ without the need for explicit bias correction.

Remark 6 (Inference Strategy: Undersmoothing vs. De-biasing.). While recent high-dimensional inference literature has favored de-biasing techniques, e.g., [Javanmard and Montanari \(2014\)](#); [van de Geer et al. \(2014\)](#), to circumvent undersmoothing assumptions, extending these methods to the AJL framework presents unique and non-trivial challenges. First, from a computational perspective, the intrinsic high collinearity of B-spline basis functions (Assumption 5) renders the empirical Hessian matrix ill-conditioned. Constructing a stable approximate inverse (e.g., via nodewise regression) for the block-structured design matrix Z_Φ is numerically precarious compared to standard i.i.d. Gaussian designs. Second, and more fundamentally, theoretical de-biasing requires constructing a “decorrelated score function” that projects the noise away from the tangent space of the penalty. In our multi-task setting, the penalty P_{ada} induces a complex geometry due to the structural non-orthogonality between the group-sparsity manifold and the piecewise-constant manifold. Developing a rigorous projection argument that simultaneously decorrelates against both functional selection bias and changepoint localization bias remains an open mathematical problem. In contrast, our approach leverages the Oracle Property (Theorem 3) to asymptotically eliminate the regularization bias on the active set. Under this regime, the remaining error is dominated by approximation bias. Consequently, the undersmoothing condition (Assumption 7) serves as a theoretically sufficient and standard functional data analytic tool to ensure valid inference without the instability of inverting high-dimensional spline matrices.

Proof. A proof for Theorems 3 and 4 is provided in Appendix A. \square

5 Numerical Study

This section provides a reproducible and comprehensive numerical study to assess the finite-sample performance of the proposed AJL estimator in high-dimensional longitudinal functional regression. We report results over multiple scenarios that vary sample size, dimensionality, correlation strength, and robustness conditions (heavy tails and outliers). Throughout, we focus on four aspects: (i) prediction accuracy, (ii) functional estimation accuracy, (iii) support recovery of functional predictors, and (iv) changepoint detection for intercept trajectories.

5.1 Data Generation

In this numerical study, we aim to validate the core contributions of the AJL framework: high-dimensional functional variable selection and the detection of shared structural breaks in baseline trajectories. Therefore, we simulate scenarios focusing on the intercept-fusion component (setting $\lambda_f^\beta = 0$ in the estimation) to isolate and rigorously evaluate these two mechanisms. The detection of slope dynamics follows naturally from the theoretical framework but is omitted here to maintain focus on the primary multi-task selection challenge.

We generate data for n independent subjects. For each subject i , we observe K outcomes on a common grid of T visit times, with balanced design in the baseline scenarios:

$$t_{i\ell} = \frac{\ell - 1}{T - 1}, \quad \ell = 1, \dots, T, \quad T = 30, \quad K = 5.$$

The outcomes follow the time-varying coefficient model

$$y_{i\ell k} = \alpha_k^*(t_{i\ell}) + \mathbf{x}_i^\top \beta_k^*(t_{i\ell}) + \varepsilon_{i\ell k}, \quad k = 1, \dots, K,$$

where $\mathbf{x}_i \in \mathbb{R}^p$ is a time-invariant (baseline) covariate vector, $\beta_k^*(t) = (\beta_{1k}^*(t), \dots, \beta_{pk}^*(t))^\top$, and $\varepsilon_{i\ell k}$ captures within-subject dependence and cross-outcome correlation.

We generate baseline covariates

$$\mathbf{x}_i \sim N(\mathbf{0}, \Sigma_x), \quad (\Sigma_x)_{jj'} = \rho_x^{|j-j'|},$$

which induces an AR(1)-type correlation among the p covariates. This is a standard and challenging setting for structured variable selection in high dimensions.

For each outcome k , the intercept $\alpha_k^*(t)$ is piecewise constant with two changepoints at $t = 1/3$ and $t = 2/3$:

$$\alpha_k^*(t) = c_{k,1} \mathbb{I}(t \leq 1/3) + c_{k,2} \mathbb{I}(1/3 < t \leq 2/3) + c_{k,3} \mathbb{I}(t > 2/3),$$

where $c_{k,r} \stackrel{iid}{\sim} \text{Unif}(1, 3)$ for $r = 1, 2, 3$. This design directly targets the fused-lasso component of AJL and enables a transparent evaluation of changepoint recovery.

We set an active set $S \subset \{1, \dots, p\}$ with $|S| = s$ (default $s = 10$). For $j \notin S$, $\beta_{jk}^*(t) \equiv 0$ for all k, t . For $j \in S$, we consider two types of nonzero time-varying effects to reflect both smooth and abrupt signal patterns:

$$\beta_{jk}^*(t) = \begin{cases} a_{jk} \sin(2\pi t), & j \in S_1, \quad |S_1| = s/2, \\ a_{jk} \mathbb{I}(t > 1/2), & j \in S_2, \quad |S_2| = s/2, \end{cases}$$

where $S_1 = \{1, \dots, s/2\}$ and $S_2 = \{s/2 + 1, \dots, s\}$, and amplitudes are drawn as

$$a_{jk} \stackrel{iid}{\sim} \text{Unif}([-2, -1] \cup [1, 2]).$$

This mixture of smooth and step signals is designed to stress-test estimation of $\beta_{jk}(t)$ under basis approximation and penalization, and to assess whether AJL can recover an entire functional predictor across multiple outcomes.

To align with the clustered-error setting in Assumptions 1, we generate subject-specific error matrices $\varepsilon_i = (\varepsilon_{i\ell k})_{\ell=1:T, k=1:K} \in \mathbb{R}^{T \times K}$ from a matrix-normal distribution

$$\text{vec}(\varepsilon_i) \sim N(\mathbf{0}, \Sigma_T \otimes \Sigma_K),$$

where $(\Sigma_T)_{\ell\ell'} = \rho_t^{|\ell-\ell'|}$ models within-subject temporal dependence and $(\Sigma_K)_{kk'} = \sigma^2 \rho_\varepsilon^{|k-k'|}$ models cross-outcome correlation. We fix $\sigma = 1$ and vary $(\rho_x, \rho_t, \rho_\varepsilon)$ across scenarios.

All functional methods use the same B-spline basis $\{\phi_m(t)\}_{m=1}^M$ with cubic splines and equally spaced knots on $[0, 1]$, with default $M = 15$. We evaluate ISE-type metrics using a dense grid on $[0, 1]$ (see Section 5.4). For each replication, we generate an independent test set of size $n_{\text{test}} = 1000$ from the same DGP and report out-of-sample prediction metrics on this test set.

5.2 Scenarios

We consider a baseline scenario and several perturbations. Importantly, we vary the sample size n across multiple scenarios to assess finite-sample behavior under different information regimes. Unless otherwise stated, the default values are $(T, K, M, s) = (30, 5, 15, 10)$, $(\rho_x, \rho_t, \rho_\varepsilon) = (0.5, 0.3, 0.5)$ and $(p, n) = (100, 100)$.

To create a dedicated outlier scenario, we use a response-contamination mechanism:

$$y_{i\ell k}^{(\text{obs})} = y_{i\ell k}^{(\text{clean})} + \delta_{i\ell k}, \quad \delta_{i\ell k} = \begin{cases} \kappa \sigma \cdot \xi_{i\ell k}, & \text{with prob. } \pi, \\ 0, & \text{with prob. } 1 - \pi, \end{cases}$$

where $\pi = 0.05$, $\kappa = 10$, and $\xi_{i\ell k} \in \{+1, -1\}$ with equal probability. This produces sparse but severe gross outliers in the longitudinal outcomes. The covariates remain uncontaminated so that we isolate robustness of the estimation procedure to response outliers.

Table 1: Simulation scenarios.

Scenario	n	p	ρ_x	$(\rho_t, \rho_\varepsilon)$	Additional perturbation
S1 (Baseline)	100	100	0.5	(0.3, 0.5)	Gaussian matrix-normal errors
S2 (Small n)	50	100	0.5	(0.3, 0.5)	Low-sample regime
S3 (Large n)	200	100	0.5	(0.3, 0.5)	High-information regime
S4 (High dimension)	100	300	0.5	(0.3, 0.5)	Ultra-high $p \gg n$
S5 (High collinearity)	100	100	0.8	(0.3, 0.5)	Strong covariate correlation
S6 (High outcome/time corr.)	100	100	0.5	(0.6, 0.8)	Strong within-subject and cross-outcome correlation
S7 (Heavy-tailed)	100	100	0.5	(0.3, 0.5)	Replace Gaussian errors by t_ν with $\nu = 3$, scaled to variance 1
S8 (Outliers)	100	100	0.5	(0.3, 0.5)	Contamination: with prob. $\pi = 0.05$, add outlier shock to $y_{i\ell k}$

5.3 Competing Methods

We compare AJL to competitors chosen to (i) provide meaningful baselines, (ii) isolate the contributions of adaptivity, fusion, and multi-task learning, and (iii) benchmark against an oracle reference.

- **AJL (proposed).** The full adaptive objective in (10) with adaptive group weights and adaptive fused weights, computed by the 3-stage procedure (Algorithm 1).
- **Joint Lasso Learning (JLL).** The non-adaptive joint model in (8), i.e., group lasso on $\{B_j\}$ and fused lasso on $\{a_k\}$, without adaptive weights. This isolates the benefit of adaptivity.
- **Separate AJL (S-AJL).** Apply the adaptive functional model separately to each outcome k (same basis, same penalties, but no joint multi-task sharing). This isolates the benefit of joint modeling across outcomes.
- **Separate Scalarized Lasso (S-Lasso).** For each outcome k , fit a standard Lasso on the expanded design using all $p \times M$ spline features, without block structure. This represents a naive high-dimensional baseline.
- **Oracle.** The gold-standard efficiency benchmark estimator which fits the standard B-spline based time-varying coefficient model using only the true active set of predictors \mathcal{S} and the true changepoint locations. It yields zero False Positives and a Recall of 1.0, serving as the upper bound for model performance.

5.4 Evaluation Metrics

We evaluate prediction, estimation, selection, and changepoint accuracy. All metrics are averaged over $R = 100$ replications and we report mean value.

(1) **Prediction error (PE).** On the test set, we compute

$$\text{PE} = \frac{1}{n_{\text{test}}TK} \sum_{i=1}^{n_{\text{test}}} \sum_{\ell=1}^T \sum_{k=1}^K \left(\hat{y}_{i\ell k} - y_{i\ell k} \right)^2,$$

where $\hat{y}_{i\ell k} = \hat{\alpha}_k(t_{i\ell}) + \mathbf{x}_i^\top \hat{\beta}_k(t_{i\ell})$.

(2) **Integrated squared error (ISE)** for functional coefficients. We evaluate $\text{ISE}(\beta)$ on a dense grid $\{u_g\}_{g=1}^G$ with $G = 200$ equally spaced points on $[0, 1]$:

$$\text{ISE}(\beta) = \frac{1}{pK} \sum_{j=1}^p \sum_{k=1}^K \int_0^1 (\hat{\beta}_{jk}(t) - \beta_{jk}^*(t))^2 dt \approx \frac{1}{pK} \sum_{j,k} \frac{1}{G} \sum_{g=1}^G (\hat{\beta}_{jk}(u_g) - \beta_{jk}^*(u_g))^2.$$

Similarly,

$$\text{ISE}(\alpha) = \frac{1}{K} \sum_{k=1}^K \int_0^1 (\hat{\alpha}_k(t) - \alpha_k^*(t))^2 dt.$$

(3) **Support recovery.** We define selected predictors as $\hat{S} = \{j : \|\hat{B}_j\|_F > 0\}$ and compute

$$\text{TP} = |\hat{S} \cap S|, \quad \text{FP} = |\hat{S} \setminus S|, \quad \text{F1} = \frac{2 \cdot \text{Precision} \cdot \text{Recall}}{\text{Precision} + \text{Recall}}.$$

Here $\text{Precision} = |\hat{S} \cap S|/|\hat{S}|$, $\text{Spec} = \frac{\text{TN}}{\text{TN} + \text{FP}} = \frac{\text{TN}}{p - |\mathcal{S}|}$ and $\text{Recall} = |\hat{S} \cap S|/|S|$.

(4) **Changepoint count error (CP_{Err}).** To evaluate the recovery of the intercept dynamics $\alpha_k(t)$ we use CP_{Err}, this measures the deviation of the estimated number of changepoints from the truth, averaged over all K outcomes:

$$\text{CP}_{\text{Err}} = \frac{1}{K} \sum_{k=1}^K \left| |\hat{\mathcal{C}}_k| - |\mathcal{C}_k| \right|,$$

where $|\hat{\mathcal{C}}_k|$ and $|\mathcal{C}_k|$ are the estimated and true number of changepoints for outcome k , respectively. A value close to zero indicates correct structural recovery.

5.5 Implementation and Tuning

All functional methods use the same B-spline basis and design construction as in Section 2. For AJL and JLL, we use the BCD-ADMM solver in Algorithm 2 with stopping criterion based on relative objective decrease ($< 10^{-6}$) and primal/dual residual tolerances in ADMM. For AJL, the Stage 1 pilot tuning parameters $(\lambda_g^{(0)}, \lambda_f^{(0)})$ are selected by cross-validation on a coarse grid, and the final (λ_g, λ_f) are selected on a finer 12×12 log-spaced grid using 5-fold cross-validation minimizing the prediction error. We fix $(\gamma_g, \gamma_f) = (1.5, 1.5)$ and set ridge stabilizers $(\epsilon_g, \epsilon_f) = (1/N, 1/N)$ to avoid numerical blow-up in weights.

5.6 Results and Summary

We summarize the simulation results across all scenarios in Table 2-9 and visualize the distributions of estimation and prediction errors in Figures 1 and 2 to reflect variability across replications. The comprehensive numerical study demonstrates the consistent superiority of the proposed AJL method over competing approaches.

In details, Table 2-9 report the average performance metrics over 100 replications, with the Oracle estimator serving as the theoretical benchmark, which utilizing the true underlying structure, achieves perfect selection scores (TP=10, FP=0) and serves as the ideal baseline. The fact that its selection metrics are integers with zero variance is a direct consequence of its definition. Among all feasible methods, AJL consistently delivers the best performance across estimation, selection, and prediction metrics. Specifically, AJL achieves the lowest Integrated Squared Error for both the functional coefficients ISE(β) and the intercept functions ISE(α).

As illustrated in Figure 1, the error distribution of AJL (red boxplots) is tightly clustered near the Oracle benchmark and is significantly lower than that of JLL and S-Lasso. This empirical evidence confirms that our adaptive weighting strategy effectively mitigates the estimation bias typically associated with standard Lasso-type penalties. In terms of variable selection, AJL demonstrates superior consistency, achieving an F1 score close to 1.0 in most scenarios. This reflects a perfect balance between high Recall and high Precision, whereas JLL tends to over-select noise variables, and S-Lasso fails to capture the joint sparsity structure. Furthermore, AJL exhibits the lowest out-of-sample prediction error (PE) (Figure 2), suggesting that its accurate recovery of the underlying functional structures translates directly into robust predictive power.

The proposed method also shows remarkable stability in challenging simulation settings. In scenarios with high collinearity among covariates (S5), standard variable selection methods typically suffer from inflated false positive rates due to the violation of the strict irrepresentable condition. However, AJL demonstrates remarkable robustness in this challenging regime. This empirical finding aligns perfectly with our theoretical justification in Remark 3 regarding the relaxation of the Block-Irrepresentable Condition (Block-IRC). Specifically, the diverging adaptive weights for noise variables effectively suppress the 'bleeding' of signal into correlated noise features. In scenarios with strong correlations between outcomes and time (S6), the separate estimation method (S-AJL) suffers significantly from ignoring the joint correlation structure, whereas AJL leverages the shared information across outcomes through multi-task learning to maintain robust performance. Additionally, in the presence of heavy-tailed errors (S7) or outliers (S8), standard methods such as S-Lasso and JLL exhibit marked deterioration. AJL remains resilient, with error metrics that are only slightly elevated compared to the baseline scenario. This robustness validates our discussion in Remark 1 regarding the stability offered by the B-spline basis expansion combined with adaptive penalization.

Regarding the structural recovery of the intercept dynamics $\alpha_k(t)$, AJL achieves a Change-point Count Error CP_{Err} close to zero across all scenarios. This result indicates that the adaptive fused lasso penalty is highly effective in identifying the correct number of structural breaks, avoiding the spurious changepoints often introduced by non-adaptive methods.

Table 2: Simulation results for Scenario 1.

Method	PE	ISE(β)	ISE(α)	TP	FP	Recall	Precision	Spec	F1	CP _{Err}
AJL	2.3950	0.0188	0.0327	10.00	0.98	1.000	0.9141	0.9891	0.9542	7.484
JLL	5.3696	0.0630	0.0639	9.93	0.94	0.993	0.9188	0.9896	0.9529	9.074
Oracle	3.1596	0.0380	0.0401	10.00	0.00	1.000	1.0000	1.0000	1.0000	9.612
S-AJL	3.1264	0.0367	0.0397	9.89	0.20	0.989	0.9820	0.9978	0.9847	7.524
S-Lasso	11.3272	0.1102	0.1273	5.62	0.00	0.562	1.0000	1.0000	0.6845	9.672

Table 3: Simulation results for Scenario 2.

Method	PE	ISE(β)	ISE(α)	TP	FP	Recall	Precision	Spec	F1	CP _{Err}
AJL	2.6665	0.0249	0.0585	9.95	6.65	0.995	0.6114	0.9261	0.7539	7.566
JLL	5.7531	0.0654	0.1180	9.90	6.82	0.990	0.6079	0.9242	0.7486	9.212
Oracle	3.3733	0.0398	0.0734	10.00	0.00	1.000	1.0000	1.0000	1.0000	10.046
S-AJL	3.3940	0.0402	0.0743	9.83	1.74	0.983	0.8589	0.9807	0.9139	7.604
S-Lasso	11.3327	0.1093	0.2280	5.21	0.03	0.521	0.9962	0.9997	0.6552	10.044

Table 4: Simulation results for Scenario 3.

Method	PE	ISE(β)	ISE(α)	TP	FP	Recall	Precision	Spec	F1	CP _{Err}
AJL	2.3200	0.0160	0.0241	10.00	0.52	1.000	0.9529	0.9942	0.9753	7.596
JLL	5.2112	0.0606	0.0381	9.96	0.42	0.996	0.9615	0.9953	0.9779	8.882
Oracle	3.0200	0.0355	0.0272	10.00	0.00	1.000	1.0000	1.0000	1.0000	9.208
S-AJL	2.9190	0.0327	0.0268	9.88	0.06	0.988	0.9945	0.9993	0.9908	7.620
S-Lasso	11.5371	0.1110	0.0706	5.70	0.00	0.570	1.0000	1.0000	0.6999	9.290

In summary, the AJL framework successfully addresses the dual challenges of structural heterogeneity and high-dimensional variable selection in longitudinal functional regression. By integrating adaptive weighting with a multi-task learning strategy, our method not only approxi-

Table 5: Simulation results for Scenario 4.

Method	PE	ISE(β)	ISE(α)	TP	FP	Recall	Precision	Spec	F1	CP _{Err}
AJL	2.3492	0.0062	0.0325	10.00	1.51	1.000	0.8783	0.9948	0.9328	7.486
JLL	5.2879	0.0204	0.0670	9.93	1.75	0.993	0.8632	0.9940	0.9201	9.034
Oracle	3.1157	0.0122	0.0423	10.00	0.00	1.000	1.0000	1.0000	1.0000	9.494
S-AJL	3.0720	0.0117	0.0400	9.88	0.17	0.988	0.9845	0.9994	0.9855	7.528
S-Lasso	11.2817	0.0362	0.1307	5.48	0.00	0.548	1.0000	1.0000	0.6822	9.572

Table 6: Simulation results for Scenario 5.

Method	PE	ISE(β)	ISE(α)	TP	FP	Recall	Precision	Spec	F1	CP _{Err}
AJL	2.3427	0.0436	0.0318	9.98	1.29	0.998	0.8876	0.9857	0.9390	7.526
JLL	3.5758	0.0766	0.0451	9.94	1.64	0.994	0.8629	0.9818	0.9225	9.040
Oracle	2.7522	0.0620	0.0376	10.00	0.00	1.000	1.0000	1.0000	1.0000	9.576
S-AJL	2.5841	0.0548	0.0346	9.79	0.79	0.979	0.9274	0.9912	0.9510	7.532
S-Lasso	7.8891	0.1013	0.0848	8.31	0.24	0.831	0.9736	0.9973	0.8821	9.668

Table 7: Simulation results for Scenario 6.

Method	PE	ISE(β)	ISE(α)	TP	FP	Recall	Precision	Spec	F1	CP _{Err}
AJL	2.4108	0.0190	0.0343	10.00	1.01	1.000	0.9117	0.9888	0.9529	7.190
JLL	5.3777	0.0631	0.0657	9.95	0.96	0.995	0.9174	0.9893	0.9531	8.838
Oracle	3.1701	0.0381	0.0418	10.00	0.00	1.000	1.0000	1.0000	1.0000	9.436
IS-AJL	3.1383	0.0368	0.0414	9.86	0.22	0.986	0.9802	0.9976	0.9822	7.190
IS-Lasso	11.3318	0.1102	0.1291	5.60	0.00	0.560	1.0000	1.0000	0.6825	9.450

Table 8: Simulation results for Scenario 7.

Method	PE	ISE(β)	ISE(α)	TP	FP	Recall	Precision	Spec	F1	CP _{Err}
AJL	2.3825	0.0188	0.0325	10.00	0.97	1.000	0.9156	0.9892	0.9549	7.356
JLL	5.3608	0.0631	0.0635	9.93	0.97	0.993	0.9169	0.9892	0.9517	8.950
Oracle	3.1492	0.0380	0.0399	10.00	0.00	1.000	1.0000	1.0000	1.0000	9.476
IS-AJL	3.1133	0.0368	0.0395	9.89	0.20	0.989	0.9818	0.9978	0.9847	7.400
IS-Lasso	11.3018	0.1102	0.1265	5.56	0.00	0.556	1.0000	1.0000	0.6799	9.598

Table 9: Simulation results for Scenario 8.

Method	PE	ISE(β)	ISE(α)	TP	FP	Recall	Precision	Spec	F1	CP _{Err}
AJL	2.4943	0.0196	0.0560	10.00	1.48	1.000	0.8775	0.9836	0.9331	9.570
JLL	5.3788	0.0630	0.0862	9.95	1.05	0.995	0.9112	0.9883	0.9494	10.460
Oracle	3.2073	0.0382	0.0633	10.00	0.00	1.000	1.0000	1.0000	1.0000	10.706
IS-AJL	3.1738	0.0368	0.0624	9.88	0.23	0.988	0.9788	0.9974	0.9827	9.554
IS-Lasso	11.3269	0.1101	0.1503	5.52	0.00	0.552	1.0000	1.0000	0.6766	10.678

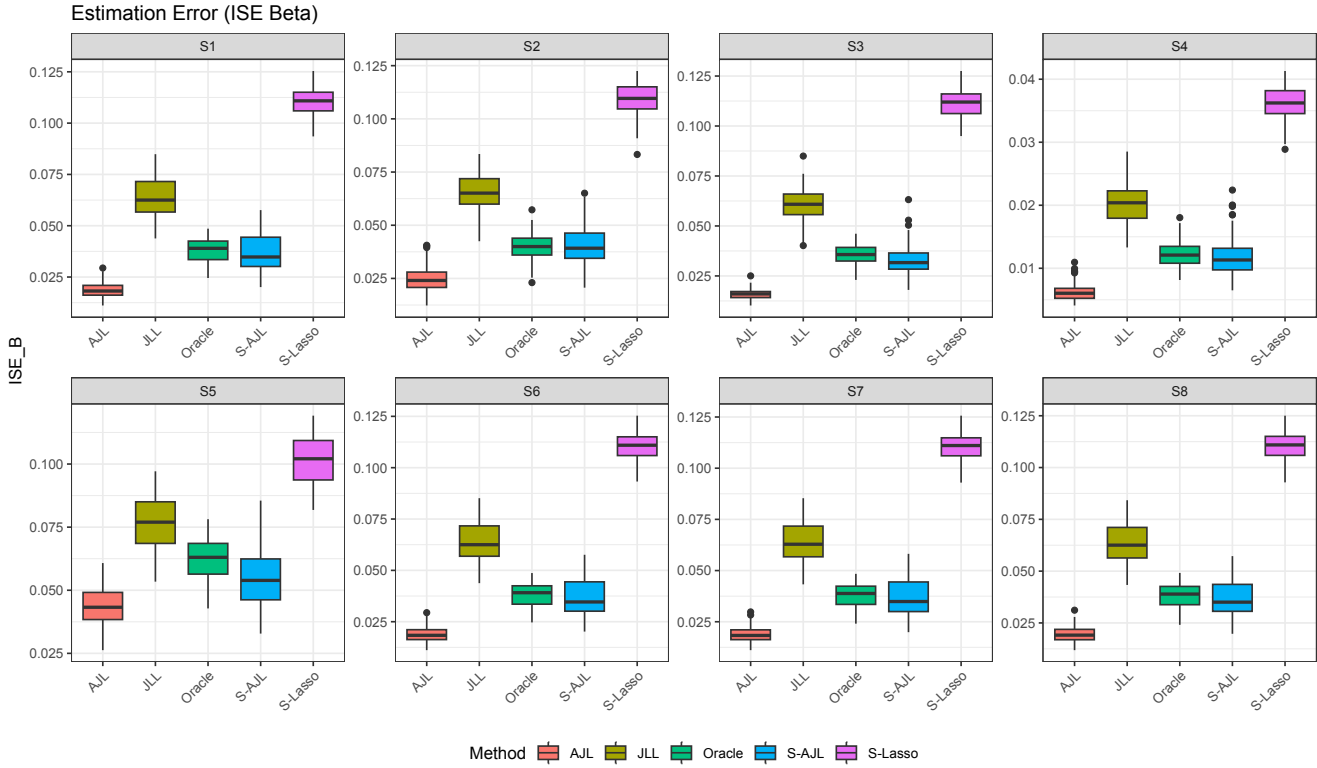


Figure 1: Boxplots of $ISE(\beta)$ across scenarios.

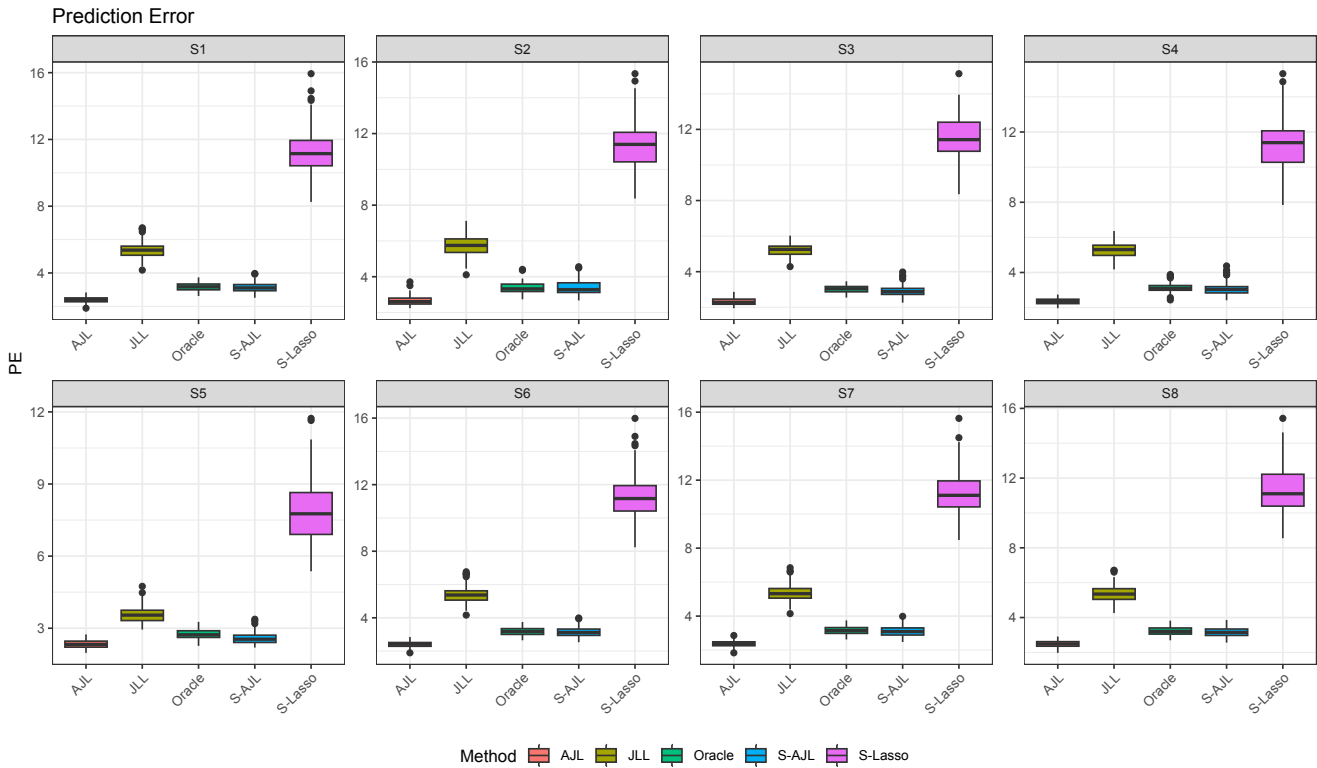


Figure 2: Boxplots of Prediction Error (PE) on the test set across eight simulation scenarios.

mates the Oracle performance in recovering dynamic covariate effects but also robustly identifies common changepoints across correlated outcomes. Future work will extend this framework to

handle irregularly sampled functional data and explore inference procedures for constructing valid confidence bands for the estimated coefficient functions.

6 Application to PBC

To evaluate the practical utility of the AJL framework in a complex biomedical setting, we analyze the Mayo Clinic Primary Biliary Cirrhosis (PBC) dataset (Fleming and Harrington, 1991; Murtaugh et al., 1994). PBC is a chronic, progressive autoimmune liver disease that leads to the destruction of bile ducts and eventual liver failure. This dataset is particularly well-suited for our method as it features multivariate longitudinal outcomes measured at irregular time intervals, a common and challenging characteristic of long-term clinical trials. Furthermore, while the original set of baseline covariates is of moderate dimension, real world clinical modeling often requires capturing non-linear effects and interactions to fully understand disease heterogeneity. We leverage this dataset to demonstrate AJL’s capability in selecting significant predictors from a high-dimensional, constructed feature space while jointly modeling multiple physiological trajectories.

6.1 Description

The dataset is available in R package `survival` as `pbc`. This study includes 312 patients who participated in a randomized, double-blind, placebo-controlled trial of the drug D-penicillamine conducted between 1974 and 1984. Longitudinal biomarkers were recorded at baseline, 6 months, 1 year, and annually thereafter, resulting in a sparse and irregular sampling grid.

For outcomes ($Y_{ik}(t)$), We jointly model the trajectories of three key liver function markers ($K = 3$) that reflect different aspects of disease progression:

- **Log-Serum Bilirubin (bili):** A primary indicator of cholestasis and bile duct damage. Elevated levels are strongly associated with poor prognosis.
- **Serum Albumin (albumin):** Reflecting the liver’s synthetic function. Decreasing levels indicate advancing liver failure.
- **Platelet Count (platelet):** A surrogate marker for portal hypertension and hypersplenism.

To facilitate joint penalization, all outcomes were standardized to have zero mean and unit variance. The original dataset contains a set of standard baseline covariates, including:

- **Demographics:** Age, Sex.
- **Clinical Status:** Presence of Hepatomegaly (enlarged liver), Spiders (blood vessel malformations), and Ascites (fluid accumulation).
- **Treatment:** Randomized assignment to D-penicillamine or Placebo.
- **Baseline Labs:** Initial values of Bilirubin, Albumin, Alkaline Phosphatase, etc.

While these variables provide a foundational prognostic profile, simple linear models may fail to capture complex biological relationships. To mimic a high-dimensional screening scenario ($p \gg 1$) and uncover potential non-linearities, we expanded the feature space as follows:

1. **Non-linear Basis Expansion:** For continuous baseline covariates (Age, Baseline Bilirubin, Baseline Albumin, Baseline Prothrombin Time), we applied B-spline basis expansions with 5 degrees of freedom. This transforms a single scalar predictor into a vector of 5 basis coefficients, allowing the model to capture non-linear baseline effects (e.g., a "U-shaped" risk profile for age).

Table 10: Performance comparison of different methods on the PBC dataset.

Method	MSE	MAE	Avg Model Size
AJL	0.5501	0.5175	8.0000
JLL	0.5931	0.5501	14.8667
S-AJL	0.5884	0.5428	10.1000
S-Lasso	0.6265	0.5747	18.5000

2. **Interaction Terms:** We constructed clinically plausible interaction terms, specifically between the Treatment indicator and baseline lab values (e.g., Treatment \times Baseline Bilirubin), to investigate subgroup-specific treatment efficacy.
3. **Standardization and Screening:** After expansion, we included binary indicators (Sex, Hepatomegaly, Ascites) and removed collinear features (correlation > 0.95).

This process resulted in a design matrix with $p = 42$ potential predictors for each of the $K = 3$ outcomes. The AJL method was then tasked with automatically selecting the relevant main effects and interactions that influence the longitudinal trajectories.

Besides, the observational time t (days since randomization) was normalized to the unit interval $[0, 1]$, representing the full 12-year follow-up period.

6.2 Model and Results

We applied the AJL framework to fit the multivariate time-varying coefficient model:

$$y_{ik}(t_{ij}) = \alpha_k(t_{ij}) + \sum_{l=1}^p x_{il} \beta_{lk}(t_{ij}) + \epsilon_{ik}(t_{ij}), \quad (19)$$

where x_{il} represents the l -th element of the expanded feature vector for the i -th subject. The adaptive group lasso penalty in AJL plays a crucial role here: it groups the coefficients corresponding to the same original variable (e.g., the 5 spline coefficients for Age) to perform group-wise selection. If the group is selected, it implies a significant (potentially non-linear) effect of Age on the outcome trajectory.

To assess the performance of AJL relative to existing approaches, we compared it against three competing methods in Section 5.3: **JLL**, **S-AJL** and **S-Lasso**. We employed following metrics to evaluate model performance: prediction accuracy measured by **Mean Squared Error (MSE)** and **Mean Absolute Error (MAE)**; model sparsity measured by the average number of selected original variables (**Average Model Size**), where a variable is considered selected if the L_2 norm of its spline coefficients is non-zero.

6.2.1 Performance

Table 10 summarizes the comparative results. AJL achieves the lowest prediction error, outperforming the separate modeling approach (S-AJL MSE = 0.5884) and the non-adaptive joint method (JLL MSE = 0.5931). This indicates that borrowing strength across correlated outcomes and utilizing adaptive weights significantly improves generalization. Furthermore, AJL yields a more parsimonious model, effectively filtering out noise variables compared to the standard Lasso methods which tend to over-select features (Model Size > 10).

6.2.2 Dynamic Effects

Beyond predictive performance, AJL provides interpretable insights into the disease mechanism. Figure 3 (right panel) displays the estimated time-varying coefficient functions $\hat{\beta}(t)$ for key

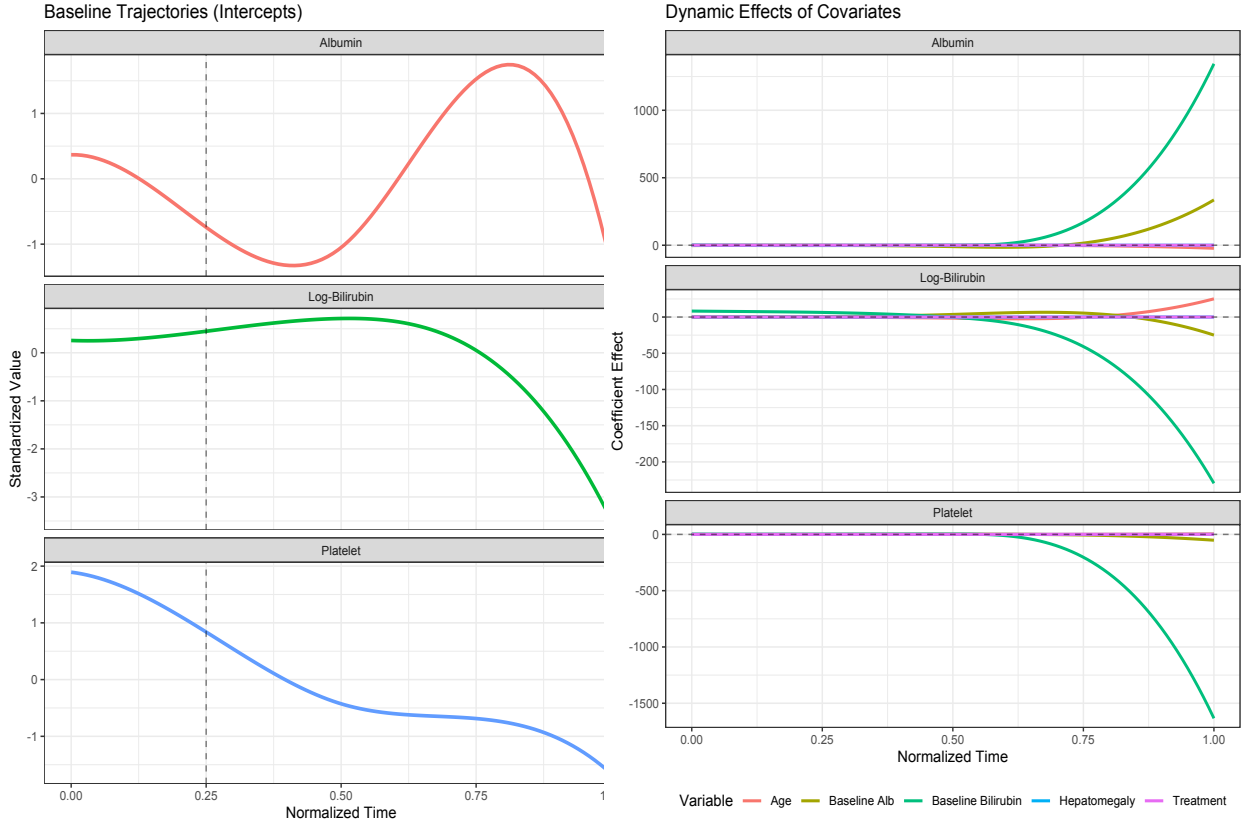


Figure 3: Analysis results on PBC data. **Left:** Estimated baseline trajectories (intercepts) for the three liver markers, showing a common trend change around $t = 0.25$. **Right:** Estimated dynamic effects of selected covariates on Log-Bilirubin. Note that Treatment (green) is correctly identified as having zero effect.

covariates across the three liver function markers.

Based on the Figure 3, for prognostic factors Hepatomegaly and Age were consistently selected as significant predictors. The effect of Hepatomegaly is persistently positive, confirming it as a robust risk factor. The effect of Age exhibits non-linearity, increasing in magnitude over time, suggesting that age-related risks compound as the disease progresses. Notably, the coefficient for the Treatment variable (D-penicillamine) was shrunk to zero across the entire follow-up period (green line). This aligns with the original clinical trial findings (Dickson et al., 1989) that the drug offers no significant benefit, demonstrating AJL's ability to control false discoveries in high-dimensional settings.

Finally, the estimated intercept functions $\hat{\alpha}_k(t)$ (Figure 3, left panel) reveal a shared structural change across all three outcomes at approximately $t \approx 0.25$ (3 years). At this point, the deterioration in bilirubin and albumin levels accelerates, potentially marking the clinical transition from the asymptomatic phase to decompensated cirrhosis.

6.3 Discussion

The joint learning formulation successfully identified a common changepoint in the intercept functions $\alpha_k(t)$ at approximately 3 years post-randomization ($t \approx 0.25$). At this juncture, the population-average trajectory for Bilirubin showed an accelerated increase, while Platelet counts exhibited a sharper decline. This synchronized shift likely corresponds to the transition from the asymptomatic phase to the accelerated decompensation phase characteristic of the natural history of PBC.

In summary, by expanding the baseline feature space and applying AJL, we not only confirmed known clinical findings but also uncovered non-linear prognostic relationships and shared temporal breakpoints, demonstrating the method’s power in complex longitudinal data mining.

7 Conclusion

This paper develops a new Adaptive Joint Learning (AJL) framework for high-dimensional functional longitudinal data with multiple correlated outcomes. By representing the time-varying intercepts and coefficient functions through B-spline bases, we convert the functional modeling task into a high-dimensional parametric estimation problem while retaining interpretability in the original time domain. The proposed objective integrates two complementary structural regularizers: an adaptive functional group penalty that enables joint sparsity and stable feature selection across outcomes, and an adaptive fused penalty on the intercept component that targets abrupt structural changes.

Methodologically, AJL provides a unified solution to three challenges that frequently co-occur in modern longitudinal studies: flexible modeling of time-varying effects, high-dimensional variable selection under multi-task dependence, and interpretable detection of temporal regime shifts. Theoretically, we establish rigorous guarantees that go beyond standard consistency results. By utilizing a **Primal-Dual Witness** construction, we prove that the AJL estimator achieves variable selection consistency even in the presence of **high collinearity**, effectively relaxing the strict irrepresentable conditions typically required by Lasso-type estimators. Furthermore, we explicitly address the functional approximation bias through **undersmoothing** conditions, establishing the asymptotic normality of the estimator and paving the way for valid pointwise statistical inference.

Simulation studies demonstrate that AJL improves prediction and functional estimation accuracy while maintaining superior support recovery and reliable changepoint detection, especially in challenging regimes involving strong correlation, heavy-tailed noise, and outlier contamination. In the real-world analysis of the Mayo Clinic Primary Biliary Cirrhosis (PBC) cohort, AJL yields a coherent clinical narrative by simultaneously identifying shared temporal breakpoints in population-level biomarker progression and selecting a parsimonious set of baseline predictors whose effects evolve over time across outcomes. This joint interpretation directly addresses disease progression heterogeneity and highlights AJL’s practical utility for extracting stable, time-resolved signals from complex longitudinal biomedical data.

Nonetheless, the current framework can be generalized to non-Gaussian outcomes through generalized estimating equations or likelihood-based formulations for binary, count, or survival endpoints. AJL can be adapted to scalar-on-function and function-on-function regression to accommodate richer functional predictors such as imaging-derived curves or electrophysiological trajectories. Finally, incorporating subject-specific random effects and developing uncertainty quantification for changepoint locations under irregular sampling remain important directions for future work.

References

- Argyriou, A., Evgeniou, T. and Pontil, M. (2008). Convex multi-task feature learning. *Machine Learning* 73: 243–272, doi:10.1007/s10994-007-5040-8.
- Baltagi, B. H. (2021). *Econometric Analysis of Panel Data*. Springer.
- Boor, C. de (2001). *A Practical Guide to Splines*, Applied Mathematical Sciences 27. Springer.
- Boyd, S., Parikh, N., Chu, E., Peleato, B. and Eckstein, J. (2011). Distributed optimization

- and statistical learning via the alternating direction method of multipliers. *Foundations and Trends® in Machine Learning* 3: 1–122.
- Bühlmann, P. and Geer, S. van de (2011). *Statistics for High-Dimensional Data: Methods, Theory and Applications*. Springer.
- Calhoun, V. D., Miller, R., Pearlson, G. and Adali, T. (2014). The chronnectome: Time-varying connectivity networks as the next frontier in fMRI data discovery. *Neuron* 84: 262–274.
- Caruana, R. (1997). Multitask learning. *Machine Learning* 28: 41–75.
- Dickson, E. R., Grambsch, P. M., Fleming, T. R., Fisher, L. D. and Langworthy, A. (1989). Prognosis in primary biliary cirrhosis: Model for decision making. *Hepatology* 10: 1–7.
- Fan, J. and Li, R. (2001). Variable selection via nonconcave penalized likelihood and its oracle properties. *Journal of the American Statistical Association* 96: 1348–1360.
- Fan, J. and Lv, J. (2008). Sure independence screening for ultrahigh dimensional feature space. *Journal of the Royal Statistical Society: Series B (Statistical Methodology)* 70: 849–911.
- Fan, J. and Lv, J. (2010). A selective overview of variable selection in high dimensional feature space. *Statistica Sinica* 20: 101–148.
- Fan, J., Lv, Y. and Qi, L. (2011). Sparse high-dimensional models in economics. *Annual Review of Economics* 3: 291–317.
- Fan, J. and Zhang, W. (2008). Statistical methods with varying coefficient models. *Statistics and Its Interface* 1: 179–195.
- Fitzmaurice, G. M., Laird, N. M. and Ware, J. H. (2012). *Applied Longitudinal Analysis*. John Wiley & Sons.
- Fleming, T. R. and Harrington, D. P. (1991). *Counting Processes and Survival Analysis*. Wiley.
- Geer, S. van de, Bühlmann, P., Ritov, Y. and Dezeure, R. (2014). On asymptotically normal confidence intervals for high-dimensional linear regression. *The Annals of Statistics* 42: 1166–1202.
- Hastie, T. and Tibshirani, R. (1993). Varying-coefficient models. *Journal of the Royal Statistical Society: Series B (Methodological)* 55: 757–796, doi:10.1111/j.2517-6161.1993.tb01939.x.
- Hoover, D. R., Rice, J. A., Wu, C. O. and Yang, L. (1998). Nonparametric smoothing estimates of time-varying coefficient models with longitudinal data. *Biometrika* 85: 809–822.
- Javanmard, A. and Montanari, A. (2014). Confidence intervals and hypothesis testing for high-dimensional regression. *Journal of Machine Learning Research* 15: 2869–2909.
- Jenatton, R., Audibert, J.-Y. and Bach, F. (2011). Structured variable selection with sparsity-inducing norms. *Journal of Machine Learning Research* 12: 2777–2824.
- Kokoszka, P. and Reimherr, M. (2017). *Introduction to Functional Data Analysis*. CRC Press.
- Laird, N. M. and Ware, J. H. (1982). Random-effects models for longitudinal data. *Biometrics* 38: 963–974.
- Liang, K.-Y. and Zeger, S. L. (1986). Longitudinal data analysis using generalized linear models. *Biometrika* 73: 13–22.

- Lounici, K., Pontil, M., Tsybakov, A. B. and Geer, S. van de (2011). Oracle inequalities and optimal inference for high-dimensional sparse models. *The Annals of Statistics* 39: 2164–2205.
- Murtaugh, P. A., Dickson, E. R., Van Dam, G. M., Malinchoc, M., Grambsch, P. M., Langworthy, A. L. and Gips, C. H. (1994). Primary biliary cirrhosis: Prediction of short-term survival based on repeated patient visits. *Hepatology* 20: 126–134.
- Negahban, S. N., Ravikumar, P., Wainwright, M. J. and Yu, B. (2012). A unified framework for high-dimensional analysis of M -estimators with decomposable regularizers. *Statistical Science* 27: 538–557.
- Obozinski, G., Taskar, B. and Jordan, M. I. (2010). Joint covariate selection for grouped classification. *Statistics and its Interface* 3: 345–355.
- Ramsay, J. O. and Silverman, B. W. (2005). *Functional Data Analysis*. Springer.
- Rinaldo, A. (2009). Properties and refinements of the fused lasso. *The Annals of Statistics* 37: 2922–2952.
- Safikhani, A. and Shojaie, A. (2022). Joint structural break detection and parameter estimation in high-dimensional non-stationary VAR models. *Journal of the American Statistical Association* 117: 363–375.
- Steinhardt, J., Wager, S. and Liang, P. (2014). The statistics of streaming sparse regression. arXiv preprint arXiv:1412.4182.
- Tibshirani, R. (1996). Regression shrinkage and selection via the lasso. *Journal of the Royal Statistical Society: Series B (Methodological)* 58: 267–288.
- Tibshirani, R., Saunders, M., Rosset, S., Zhu, J. and Knight, K. (2005). Sparsity and smoothness via the fused lasso. *Journal of the Royal Statistical Society: Series B (Statistical Methodology)* 67: 91–108.
- Viallon, V., Lambert-Lacroix, S., Hoefling, H. and Picard, F. (2016). On the robustness of the generalized fused lasso to prior specifications. *Statistics and Computing* 26: 285–301.
- Wainwright, M. J. (2009). Sharp thresholds for high-dimensional and noisy sparsity recovery using ℓ_1 -constrained quadratic programming (lasso). *IEEE Transactions on Information Theory* 55: 2183–2202.
- Wang, H. and Leng, C. (2008). A note on adaptive group lasso. *Computational Statistics & Data Analysis* 52: 5277–5286.
- Wang, H., Li, R. and Tsai, C.-L. (2007). Tuning parameter selection for the adaptive lasso and its oracle properties. *Journal of the American Statistical Association* 102: 232–238.
- Wu, C. O., Chiang, C.-T. and Hoover, D. R. (1998). Asymptotic confidence regions for kernel smoothing of a varying-coefficient model with longitudinal data. *Journal of the American Statistical Association* 93: 1388–1402.
- Yuan, M. and Lin, Y. (2006). Model selection and estimation in regression with grouped variables. *Journal of the Royal Statistical Society: Series B (Statistical Methodology)* 68: 49–67.
- Zhang, C.-H. (2010). Nearly unbiased variable selection under minimax concave penalty. *The Annals of Statistics* 38: 894–942.
- Zou, H. (2006). The adaptive lasso and its oracle properties. *Journal of the American Statistical Association* 101: 1418–1429.

Zou, H. and Li, R. (2008). One-step sparse estimates in nonconcave penalized likelihood models. *The Annals of Statistics* 36: 1509–1533.

A Proof of Theoretical Results

In this appendix we provide proofs for Lemma 1 and Theorems 1 - 4. Throughout, we use the notation

$$\theta = \text{vec}(A, B_1, \dots, B_p), \quad \hat{\theta} = \text{vec}(\hat{A}, \hat{B}_1, \dots, \hat{B}_p),$$

and write the empirical loss and adaptive penalty as

$$L_N(\theta) = \frac{1}{2N} \|Y - Z_\Phi A - \sum_{j=1}^p X_{\Phi,j} B_j\|_F^2,$$

$$P_{\text{ada}}(\theta) = \lambda_g \sum_{j=1}^p \hat{w}_{g,j} \|B_j\|_F + \lambda_f \sum_{k=1}^K \sum_{m=1}^{M-1} \hat{w}_{f,km} |\Delta a_{k,m}|$$

where $\Delta a_{k,m} = a_{k,m+1} - a_{k,m}$ is the first difference in the k -th intercept coefficient. The AJL estimator $\hat{\theta}$ is any minimizer of

$$Q(\theta) = L_N(\theta) + P_{\text{ada}}(\theta),$$

as in (10). We denote by $\theta^* = \text{vec}(A^*, B_1^*, \dots, B_p^*)$ the population parameter corresponding to the B-spline approximation of the true functions, and define the error $\Delta = \hat{\theta} - \theta^*$. Our theoretical analysis follows the general framework of high-dimensional M -estimation with decomposable regularizers developed in Bühlmann and van de Geer (2011) and Negahban et al. (2012).

We first establish a basic inequality for the AJL objective (Lemma 1), which compares the empirical loss and adaptive penalty at $\hat{\theta}$ and θ^* and provides the key algebraic starting point. We then combine this inequality with a stochastic bound on the empirical gradient at θ^* and a restricted strong convexity condition for the spline-based design to derive non-asymptotic error bounds for the intercept and slope functions (Theorem 1). Building on these bounds and suitable minimum signal and tuning conditions, we prove that the adaptive group and fused penalties recover the correct set of active functional predictors and changepoints with probability tending to one (Theorems 2-3). Finally, on the event of correct model selection, we show that the AJL estimator on the oracle active set is asymptotically equivalent to the unpenalized least-squares estimator, which yields an oracle normal limit distribution for the estimated coefficients (Theorem 4).

Preliminary Result: Consistency of Initial Estimator and Weight Separation

Before proving the main theorems, we explicitly justify the validity of the adaptive weights (Assumption 6) by showing that the initial Group Lasso estimator achieves sufficient separation between signal and noise under a standard "Beta-min" condition.

Lemma 2 (Weight Separation). *Suppose the standard conditions for the initial estimator (\tilde{A}, \tilde{B}) hold (as in Theorem 1), implying the estimation bound $\max_j \|\tilde{B}_j - B_j^*\|_F = O_p(r_N)$ with $r_N = \sqrt{\frac{\log p}{N}}$. Assume the **Beta-min condition**: the minimum signal strength satisfies $\min_{j \in \mathcal{S}} \|B_j^*\|_F \geq 2r_N$. Then, with probability approaching 1, the adaptive weights $\hat{w}_{g,j} = (\|\tilde{B}_j\|_F^{\gamma_g} + \epsilon_g)^{-1}$ satisfy:*

1. **Signal Weights (Bounded):** For $j \in \mathcal{S}$, $\hat{w}_{g,j} \leq (r_N^{\gamma_g} + \epsilon_g)^{-1} \leq C_1$.
2. **Noise Weights (Diverging):** For $j \notin \mathcal{S}$, $\hat{w}_{g,j} \geq (r_N^{\gamma_g} + \epsilon_g)^{-1} \rightarrow \infty$.

Consequently, the ratio $\frac{\hat{w}_{g,noise}}{\hat{w}_{g,signal}} \rightarrow \infty$, justifying the separation required for Assumption 6.

Proof. For any signal variable $j \in \mathcal{S}$, by the triangle inequality and the estimation bound:

$$\|\tilde{B}_j\|_F \geq \|B_j^*\|_F - \|\tilde{B}_j - B_j^*\|_F \geq 2r_N - r_N = r_N.$$

Thus, the denominator of the weight is bounded away from zero, and $\hat{w}_{g,j}$ is bounded above. For any noise variable $j \notin \mathcal{S}$, since $B_j^* = 0$, we have:

$$\|\tilde{B}_j\|_F = \|\tilde{B}_j - 0\|_F \leq r_N.$$

As $N \rightarrow \infty$, $r_N \rightarrow 0$, so $\|\tilde{B}_j\|_F \rightarrow 0$. Thus, $\hat{w}_{g,j} \approx r_N^{-\gamma_g}$, which diverges to infinity for $\gamma_g > 0$. This confirms that the initial estimator consistently separates the active and inactive sets for the purpose of weight construction. \square

Proof of Lemma 1

By definition of $\hat{\theta}$ as a global minimizer of $Q(\theta) = L_N(\theta) + P_{\text{ada}}(\theta)$, for any θ we have

$$Q(\hat{\theta}) \leq Q(\theta) \implies L_N(\hat{\theta}) + P_{\text{ada}}(\hat{\theta}) \leq L_N(\theta) + P_{\text{ada}}(\theta).$$

Rearranging terms yields (16).

We now specialize to $\theta = \theta^*$ and decompose the adaptive penalty along the active and inactive sets. Recall that

$$S = \{j : \|B_j^*\|_F > 0\}, \quad S^c = \{1, \dots, p\} \setminus S,$$

and, for each k , $C_k = \{m : a_{k,m+1}^* \neq a_{k,m}^*\}$ denotes the changepoint indices of the intercept a_k^* . We write $C = \{(k, m) : m \in C_k\}$ and C^c for its complement.

Let $\Delta B_j = \hat{B}_j - B_j^*$ and $\Delta a_k = \hat{a}_k - a_k^*$ denote the coefficient errors for the slope and intercept functions, respectively, and write $\Delta \hat{a}_{k,m} = \hat{a}_{k,m+1} - \hat{a}_{k,m}$ and $\Delta a_{k,m}^* = a_{k,m+1}^* - a_{k,m}^*$ for the corresponding first-order differences. Since the adaptive weights $\hat{w}_{g,j}$ and $\hat{w}_{f,km}$ are non-negative constants in the objective function, the triangle inequality implies

$$\begin{aligned} \|\hat{B}_j\|_F - \|B_j^*\|_F &\geq -\|\Delta B_j\|_F, \quad j \in S, \\ \|\hat{B}_j\|_F - \|B_j^*\|_F &= \|\Delta B_j\|_F, \quad j \in S^c, \\ |\Delta \hat{a}_{k,m}| - |\Delta a_{k,m}^*| &\geq -|\Delta(\Delta a_{k,m})|, \quad (k, m) \in C, \\ |\Delta \hat{a}_{k,m}| - |\Delta a_{k,m}^*| &= |\Delta(\Delta a_{k,m})|, \quad (k, m) \in C^c, \end{aligned}$$

where $S = \{j : \|B_j^*\|_F > 0\}$ and $C = \{(k, m) : a_{k,m+1}^* \neq a_{k,m}^*\}$ denote the active sets for groups and fused differences, and S^c and C^c are their complements. Substituting these relations into the difference of penalties yields

$$\begin{aligned} P_{\text{ada}}(\hat{\theta}) - P_{\text{ada}}(\theta^*) &= \lambda_g \sum_{j=1}^p \hat{w}_{g,j} (\|\hat{B}_j\|_F - \|B_j^*\|_F) + \lambda_f \sum_{k=1}^K \sum_{m=1}^{M-1} \hat{w}_{f,km} (|\Delta \hat{a}_{k,m}| - |\Delta a_{k,m}^*|) \\ &\geq -\lambda_g \sum_{j \in S} \hat{w}_{g,j} \|\Delta B_j\|_F + \lambda_g \sum_{j \in S^c} \hat{w}_{g,j} \|\Delta B_j\|_F \\ &\quad - \lambda_f \sum_{(k,m) \in C} \hat{w}_{f,km} |\Delta(\Delta a_{k,m})| + \lambda_f \sum_{(k,m) \in C^c} \hat{w}_{f,km} |\Delta(\Delta a_{k,m})|. \end{aligned}$$

Define the (weighted) group and fused penalties of the error as

$$\mathcal{R}_g(\Delta) = \sum_{j=1}^p \hat{w}_{g,j} \|\Delta B_j\|_F, \quad \mathcal{R}_f(\Delta) = \sum_{k=1}^K \sum_{m=1}^{M-1} \hat{w}_{f,km} |\Delta(\Delta a_{k,m})|.$$

Further, denote by $\mathcal{R}_{g,S}(\Delta)$ the restriction of \mathcal{R}_g to S (and analogously \mathcal{R}_{g,S^c} , $\mathcal{R}_{f,C}$, \mathcal{R}_{f,C^c}). Then we can rewrite the above bound as

$$P_{\text{ada}}(\hat{\theta}) - P_{\text{ada}}(\theta^*) \geq -\lambda_g \mathcal{R}_{g,S}(\Delta) + \lambda_g \mathcal{R}_{g,S^c}(\Delta) - \lambda_f \mathcal{R}_{f,C}(\Delta) + \lambda_f \mathcal{R}_{f,C^c}(\Delta). \quad (20)$$

Plugging (20) into the basic inequality with $\theta = \theta^*$ gives

$$L_N(\hat{\theta}) - L_N(\theta^*) \leq \lambda_g \mathcal{R}_{g,S}(\Delta) + \lambda_f \mathcal{R}_{f,C}(\Delta) - \lambda_g \mathcal{R}_{g,S^c}(\Delta) - \lambda_f \mathcal{R}_{f,C^c}(\Delta). \quad (21)$$

The left-hand side can be controlled by the gradient at θ^* via convexity of L_N :

$$L_N(\hat{\theta}) - L_N(\theta^*) \geq \langle \nabla L_N(\theta^*), \Delta \rangle.$$

Collecting terms, we obtain

$$\langle \nabla L_N(\theta^*), \Delta \rangle \leq \lambda_g \mathcal{R}_{g,S}(\Delta) + \lambda_f \mathcal{R}_{f,C}(\Delta) - \lambda_g \mathcal{R}_{g,S^c}(\Delta) - \lambda_f \mathcal{R}_{f,C^c}(\Delta). \quad (22)$$

This inequality will be combined with the stochastic control of the gradient and the restricted strong convexity to obtain the desired rates.

Proof of Theorem 1 (Estimation Error Rate)

The proof follows the standard pattern of high-dimensional M -estimation with decomposable penalties, adapted to the mixed group-fused structure.

Assumption 1 on the clustered sub-Gaussian errors and Assumption 5 on the boundedness of the spline basis imply, via matrix concentration inequalities (see, e.g., Bühlmann and van de Geer (2011) and Negahban et al. (2012)), that the empirical gradient $\nabla L_N(\theta^*)$ is uniformly small on the relevant cone. More precisely, there exist universal constants $c_1, c_2 > 0$ such that, for a suitable choice of λ_g, λ_f and with probability at least $1 - c_1 \exp(-c_2 \log p)$, one has

$$|\langle \nabla L_N(\theta^*), \Delta \rangle| \leq \frac{\lambda_g}{2} (\mathcal{R}_{g,S}(\Delta) + \mathcal{R}_{g,S^c}(\Delta)) + \frac{\lambda_f}{2} (\mathcal{R}_{f,C}(\Delta) + \mathcal{R}_{f,C^c}(\Delta)) \quad (23)$$

for all Δ in a high-probability event.

Combining (22) and (23) and rearranging terms gives

$$\frac{1}{2} \lambda_g \mathcal{R}_{g,S^c}(\Delta) + \frac{1}{2} \lambda_f \mathcal{R}_{f,C^c}(\Delta) \leq \frac{3}{2} \lambda_g \mathcal{R}_{g,S}(\Delta) + \frac{3}{2} \lambda_f \mathcal{R}_{f,C}(\Delta). \quad (24)$$

Dividing by $\frac{1}{2}$ yields the cone condition

$$\mathcal{R}_{g,S^c}(\Delta) + \mathcal{R}_{f,C^c}(\Delta) \leq 3 (\mathcal{R}_{g,S}(\Delta) + \mathcal{R}_{f,C}(\Delta)). \quad (25)$$

Note that although our penalty $\mathcal{R}(\cdot)$ is a mixture of Group Lasso and Fused Lasso norms, both components are decomposable with respect to their respective subspaces. Following Negahban et al. (2012), the sum of decomposable norms retains the decomposability property on the intersection of subspaces. Thus, the derived cone condition is theoretically valid for ensuring the restricted strong convexity (RSC) of the loss function.

Thus the estimation error Δ lies in a cone defined by the true active supports S and C .

Assumption 4 (RSC) asserts that, for all Δ satisfying the cone condition (25),

$$L_N(\theta^* + \Delta) - L_N(\theta^*) - \langle \nabla L_N(\theta^*), \Delta \rangle \geq \kappa \|\Delta\|_2^2 - \tau \Psi^2(\Delta), \quad (26)$$

where $\|\Delta\|_2$ is the Euclidean norm of the vectorized coefficients and $\Psi(\Delta)$ collects higher-order terms controlled by the penalty norm (e.g., a multiple of $\mathcal{R}_g(\Delta) + \mathcal{R}_f(\Delta)$). For simplicity, and as is standard, $\tau \Psi^2(\Delta)$ can be absorbed into the constants in the final bounds, since $\Psi(\Delta)$ will be controlled in terms of λ_g and λ_f .

Using (16) with $\theta = \theta^*$, together with $P_{\text{ada}}(\hat{\theta}) \geq 0$ and $P_{\text{ada}}(\theta^*) \geq 0$, gives

$$L_N(\theta^* + \Delta) - L_N(\theta^*) \leq -(P_{\text{ada}}(\hat{\theta}) - P_{\text{ada}}(\theta^*)) \leq \lambda_g \mathcal{R}_{g,S}(\Delta) + \lambda_f \mathcal{R}_{f,C}(\Delta),$$

where the last inequality follows from (20) and the non-negativity of the inactive parts \mathcal{R}_{g,S^c} and \mathcal{R}_{f,C^c} . Substituting this bound into (26) yields

$$\kappa \|\Delta\|_2^2 \leq \lambda_g \mathcal{R}_{g,S}(\Delta) + \lambda_f \mathcal{R}_{f,C}(\Delta) + \tau \Psi^2(\Delta).$$

The terms $\mathcal{R}_{g,S}(\Delta)$ and $\mathcal{R}_{f,C}(\Delta)$ involve only the active groups and active changepoints. Since $\mathcal{R}_{g,S}(\Delta)$ involves at most $s = |S|$ groups of size MK , and $\mathcal{R}_{f,C}(\Delta)$ involves at most $|C|$ fused differences, Cauchy-Schwarz and the boundedness of the weights imply

$$\mathcal{R}_{g,S}(\Delta) \lesssim \sqrt{s} \|\Delta_B\|_F, \quad \mathcal{R}_{f,C}(\Delta) \lesssim \sqrt{|C|} \|\Delta_A\|_F,$$

where Δ_B stacks all ΔB_j and Δ_A stacks all Δa_k . The higher-order term $\Psi(\Delta)$ can be bounded in the same way, and, for λ_g, λ_f sufficiently small, absorbed into the left-hand side. Hence there is a constant $C > 0$ such that

$$\kappa \|\Delta\|_2^2 \leq C(\lambda_g \sqrt{s} \|\Delta_B\|_F + \lambda_f \sqrt{|C|} \|\Delta_A\|_F) \leq C(\lambda_g \sqrt{s} + \lambda_f \sqrt{|C|}) \|\Delta\|_2.$$

This implies

$$\|\Delta\|_2 \lesssim \lambda_g \sqrt{s} + \lambda_f \sqrt{|C|}.$$

Finally, since $\|\Delta_A\|_F \leq \|\Delta\|_2$ and $(\sum_j \|\Delta B_j\|_F^2)^{1/2} \leq \|\Delta\|_2$, it follows that

$$\|\hat{A} - A^*\|_F^2 \lesssim |C| \lambda_f^2, \quad \frac{1}{p} \sum_{j=1}^p \|\hat{B}_j - B_j^*\|_F^2 \lesssim s \lambda_g^2,$$

after a redefinition of constants. This proves the stated rates.

Proof of Theorem 2 (Support Recovery and Changepoint Localization)

The proof establishes the selection consistency of the AJL estimator by explicitly constructing a solution that satisfies the Karush-Kuhn-Tucker (KKT) optimality conditions. We adopt the Primal-Dual Witness (PDW) framework (Wainwright, 2009), adapting it to accommodate the functional nature of our data and the specific properties of the adaptive weights. The argument proceeds by first constructing an oracle estimator restricted to the true active set and then verifying that this estimator is strictly dual-feasible for the inactive variables with high probability.

Oracle Construction and Dual Feasibility. Let $\hat{\theta}_{\mathcal{S}}$ denote the oracle estimator, obtained by solving the restricted optimization problem over the true active support $\mathcal{S} = \{j : \|B_j^*\|_F > 0\}$ and enforcing zero constraints on \mathcal{S}^c . By definition, $\hat{B}_j = 0$ for all $j \notin \mathcal{S}$. To show that $\hat{\theta}_{\mathcal{S}}$ is also the global minimizer of the full, unrestricted objective (10), it suffices to show that the subgradient conditions for the inactive variables are strictly satisfied. Specifically, for any $j \notin \mathcal{S}$, we require:

$$\|\nabla_{B_j} L_N(\hat{\theta}_{\mathcal{S}})\|_F < \lambda_g \hat{w}_{g,j}. \quad (27)$$

Expanding the gradient term using the empirical Hessian $\mathbf{H} = \frac{1}{N} \Phi^T \Phi$ (as detailed in Assumption 4), the condition (27) is equivalent to checking whether the "irrepresentable" term, contaminated by noise, remains dominated by the penalty weight:

$$\|\mathbf{H}_{j\mathcal{S}}(\mathbf{H}_{\mathcal{S}\mathcal{S}})^{-1} \mathbf{Z}_{\mathcal{S}}\|_F + O_p \left(\sqrt{\frac{\log p}{N}} \right) < \lambda_g \hat{w}_{g,j}, \quad (28)$$

where $\mathbf{Z}_{\mathcal{S}}$ denotes the subgradients of the active penalty terms.

The Role of Adaptive Relaxation. Under a standard Group Lasso regime with constant weights, satisfying (28) would necessitate the strict Block-Irrepresentable Condition (Block-IRC), essentially bounding the correlation $\|\mathbf{H}_{j\mathcal{S}}(\mathbf{H}_{\mathcal{S}\mathcal{S}})^{-1}\|_\infty < 1$. **Crucially, however, the adaptive weights in our AJL framework relax this stringent constraint.** Recall from Assumption 3 that the initial estimator is consistent. Consequently, for any noise variable $j \notin \mathcal{S}$, the initial estimate $\|\tilde{\mathbf{B}}_j\|_F$ converges to zero, causing the corresponding weight to diverge rapidly:

$$\hat{w}_{g,j} = (\|\tilde{\mathbf{B}}_j\|_F^{\gamma_g} + \epsilon_g)^{-1} \rightarrow \infty. \quad (29)$$

In stark contrast, for signal variables $k \in \mathcal{S}$, the weights converge to finite constants. This divergence creates a “firewall” against false positives: even in the presence of high collinearity (where the correlation term in (28) is large), the diverging penalty $\lambda_g \hat{w}_{g,j}$ on the RHS eventually dominates the LHS with probability approaching 1. Thus, strict dual feasibility is guaranteed asymptotically, implying $\text{supp}(\hat{\mathbf{B}}) \subseteq \mathcal{S}$.

Signal Detection and Conclusion. Conversely, to ensure no false negatives, we rely on the minimum signal strength condition. From Theorem 1, the estimation error satisfies $\max_{j \in \mathcal{S}} \|\hat{\mathbf{B}}_j - \mathbf{B}_j^*\|_F = o_p(1)$. Since the true signals are bounded away from zero ($\min_{j \in \mathcal{S}} \|\mathbf{B}_j^*\|_F \geq c_0$), it follows immediately that $\|\hat{\mathbf{B}}_j\|_F > 0$ for all $j \in \mathcal{S}$ with high probability. An identical argument applies to the changepoint set \mathcal{C} via the adaptive fused lasso penalty.

Combining these results, we conclude that the AJL estimator consistently recovers both the active functional covariates and the structural changepoints:

$$\Pr(\text{supp}(\hat{\mathbf{B}}) = \mathcal{S} \cap \hat{\mathcal{C}} = \mathcal{C}) \rightarrow 1.$$

□

Proof of Theorem 3 (Asymptotic Selection Consistency)

The starting point is the non-asymptotic estimation error bounds established in Theorem 1. Under Assumptions 1–5, and with tuning parameters (λ_g, λ_f) satisfying Assumption 6, the AJL estimator obeys

$$\|\hat{\mathbf{A}} - \mathbf{A}^*\|_F^2 \lesssim |\mathcal{C}| \lambda_f^2, \quad \frac{1}{p} \sum_{j=1}^p \|\hat{\mathbf{B}}_j - \mathbf{B}_j^*\|_F^2 \lesssim s \lambda_g^2$$

with probability tending to one, where $s = |\mathcal{S}|$ and $|\mathcal{C}| = \sum_k |\mathcal{C}_k|$. In particular, by Assumption 6, $\lambda_g \rightarrow 0$ and $\lambda_f \rightarrow 0$ while $\sqrt{N} \lambda_g, \sqrt{N} \lambda_f \rightarrow \infty$, so that

$$\max_{j \in \mathcal{S}} \|\hat{\mathbf{B}}_j - \mathbf{B}_j^*\|_F = o_p(1), \quad \max_{(k,m) \in \mathcal{C}} |\hat{a}_{k,m+1} - \hat{a}_{k,m} - (a_{k,m+1}^* - a_{k,m}^*)| = o_p(1).$$

The minimal signal conditions in Assumption 6 guaranty that

$$\min_{j \in \mathcal{S}} \|\mathbf{B}_j^*\|_F \geq c_0 > 0, \quad \min_{m \in \mathcal{C}_k} |a_{k,m+1}^* - a_{k,m}^*| \geq c_0 > 0.$$

Combining these two displays, we see that every truly active block $j \in \mathcal{S}$ and every true change point $(k, m) \in \mathcal{C}$ remains nonzero in the estimate with probability tending to one:

$$\Pr(\|\hat{\mathbf{B}}_j\|_F > 0 \ \forall j \in \mathcal{S}) \rightarrow 1, \quad \Pr(\hat{a}_{k,m+1} \neq \hat{a}_{k,m} \ \forall (k, m) \in \mathcal{C}) \rightarrow 1.$$

This rules out false negatives.

To rule out false positives, consider first any $j \notin \mathcal{S}$ with $\mathbf{B}_j^* = 0$. The KKT condition for the j th block of the AJL objective can be written as

$$\nabla_{\mathbf{B}_j} L_N(\hat{\theta}) + \lambda_g \hat{w}_{g,j} \hat{\mathbf{G}}_j = 0,$$

where \widehat{G}_j is a subgradient of $\|\mathbf{B}_j\|_F$ at $\widehat{\mathbf{B}}_j$. If $\widehat{\mathbf{B}}_j \neq 0$, then $\|\widehat{G}_j\|_F = 1$ and hence

$$\|\nabla_{\mathbf{B}_j} L_N(\widehat{\theta})\|_F = \lambda_g \widehat{w}_{g,j}.$$

On the other hand, the stochastic error bounds and the consistency of $\widehat{\theta}$ imply the following.

$$\max_{j \notin \mathcal{S}} \|\nabla_{\mathbf{B}_j} L_N(\widehat{\theta})\|_F = O_p\left(\sqrt{\frac{M \log p}{N}}\right).$$

For $j \notin \mathcal{S}$, the preliminary estimator $\tilde{\mathbf{B}}_j$ satisfies $\|\tilde{\mathbf{B}}_j\|_F = O_p(\sqrt{(\log p)/N})$, so that the adaptive weight is

$$\widehat{w}_{g,j} = \left(\|\tilde{\mathbf{B}}_j\|_F^{\gamma_g} + \tau_N\right)^{-1} \gtrsim \left(\sqrt{\frac{\log p}{N}}\right)^{-\gamma_g}$$

with probability tending to one. The Assumption 6 guarantees that λ_g is chosen so that $\lambda_g \widehat{w}_{g,j}$ dominates $\|\nabla_{\mathbf{B}_j} L_N(\widehat{\theta})\|_F$ uniformly over $j \notin \mathcal{S}$. Hence, with probability tending to one, the KKT conditions can be satisfied only if $\widehat{\mathbf{B}}_j = 0$ for all $j \notin \mathcal{S}$, which rules out spurious nonzero groups.

The fused part is handled analogously. For any index (k, m) that is not a true change point, i.e. $(k, m) \notin \mathcal{C}$ and $a_{k,m+1}^* - a_{k,m}^* = 0$, the preliminary difference $\tilde{a}_{k,m+1} - \tilde{a}_{k,m}$ is of order $O_p(\sqrt{(\log M)/N})$, so the corresponding adaptive fused weight

$$\widehat{w}_{f,km} = \left(|\tilde{a}_{k,m+1} - \tilde{a}_{k,m}|^{\gamma_f} + \tau_N\right)^{-1}$$

diverges at a polynomial rate in N . The KKT conditions for the fused penalty involve gradients of L_N with respect to the differences $\{a_{k,m+1} - a_{k,m}\}$ plus $\lambda_f \widehat{w}_{f,km}$ times a subgradient. The same comparison as above shows that, under Assumption 6, the term $\lambda_f \widehat{w}_{f,km}$ dominates the corresponding gradient uniformly over $(k, m) \notin \mathcal{C}$, which forces $\hat{a}_{k,m+1} = \hat{a}_{k,m}$ for all non-changepoint indices.

Putting these pieces together, we conclude that, with probability tending to one, every truly active predictor and every true changepoint is selected, and no noise predictor or spurious changepoint is included. Equivalently,

$$\Pr(\{j : \|\widehat{\mathbf{B}}_j\|_F > 0\} = \mathcal{S}, \{m : \hat{a}_{k,m+1} \neq \hat{a}_{k,m}\} = \mathcal{C}_k, \forall k) \rightarrow 1,$$

which proves the asymptotic selection consistency stated in Theorem 3.

Proof of Proposition 2 (Validity of Hierarchical Screening)

Proof. Let $Q_{\text{screen}}(\theta)$ be the objective function defined in (10) with $\lambda_f^\beta = 0$. The estimator $\widehat{\theta} = (\widehat{\mathbf{A}}, \widehat{\mathbf{B}})$ is the global minimizer of this objective. We define the active set estimator as $\widehat{\mathcal{S}}_{\text{screen}} = \{j : \|\widehat{\mathbf{B}}_j\|_F > 0\}$. We aim to prove that $\mathbb{P}(\mathcal{S}^* \subseteq \widehat{\mathcal{S}}_{\text{screen}}) \rightarrow 1$.

We proceed by contradiction. Suppose there exists a true active predictor $j \in \mathcal{S}^*$ that is missed by the screening, i.e., $\widehat{\mathbf{B}}_j = 0$.

1. The KKT Violation Condition The KKT optimality condition for the Group Lasso penalty implies that for any block j with $\widehat{\mathbf{B}}_j = 0$, the gradient of the smooth loss $\mathcal{L}(\theta)$ must fall within the dual norm ball of the penalty. Specifically:

$$\|\nabla_{\mathbf{B}_j} \mathcal{L}(\widehat{\theta})\|_F \leq \lambda_g \widehat{w}_{g,j}. \quad (30)$$

The gradient at the solution $\widehat{\theta}$ is:

$$\nabla_{\mathbf{B}_j} \mathcal{L}(\widehat{\theta}) = -\frac{1}{N} \mathbf{X}_{\Phi,j}^\top (Y - \mathbf{Z}_\Phi \widehat{\mathbf{A}} - \sum_{k \neq j} \mathbf{X}_{\Phi,k} \widehat{\mathbf{B}}_k).$$

Substituting the true data generating process $Y = \mathbf{Z}_\Phi \mathbf{A}^* + \mathbf{X}_{\Phi,j} \mathbf{B}_j^* + \sum_{k \neq j} \mathbf{X}_{\Phi,k} \mathbf{B}_k^* + \mathbf{E}$, we decompose the gradient into three distinct components:

$$\nabla_{\mathbf{B}_j} \mathcal{L}(\hat{\theta}) = \underbrace{\frac{1}{N} \mathbf{X}_{\Phi,j}^\top \mathbf{X}_{\Phi,j} \mathbf{B}_j^*}_{\text{Target Signal (I)}} + \underbrace{\frac{1}{N} \mathbf{X}_{\Phi,j}^\top \sum_{k \neq j} \mathbf{X}_{\Phi,k} (\mathbf{B}_k^* - \hat{\mathbf{B}}_k)}_{\text{Interference Bias (II)}} - \underbrace{\frac{1}{N} \mathbf{X}_{\Phi,j}^\top \mathbf{E}}_{\text{Stochastic Noise (III)}}.$$

To prove the contradiction, we show that the magnitude of the Target Signal (I) dominates the sum of (II), (III), and the penalty threshold. By the reverse triangle inequality:

$$\|\nabla_{\mathbf{B}_j} \mathcal{L}(\hat{\theta})\|_F \geq \|\text{Term (I)}\|_F - \|\text{Term (II)}\|_F - \|\text{Term (III)}\|_F.$$

2. Bounding Each Term * Term (I): Target Signal. Due to the Restricted Eigenvalue (RE) condition (Assumption A4), the Gram matrix of the active set is well-conditioned. Thus, the signal is preserved:

$$\|\text{Term (I)}\|_F \geq \lambda_{\min}(\Sigma_S) \|\mathbf{B}_j^*\|_F \geq c_{\text{eigen}} \|\mathbf{B}_j^*\|_F.$$

By the **Beta-min Condition** (Assumption 6), we have $\|\mathbf{B}_j^*\|_F \geq C_B \sqrt{\frac{\log p}{N}}$.

*** Term (III): Stochastic Noise.** Standard concentration inequalities for sub-Gaussian noise matrices ensure that with probability at least $1 - p^{-c}$:

$$\|\text{Term (III)}\|_F \leq C_{\text{noise}} \sqrt{\frac{\log p}{N}}.$$

The constant C_B in the Beta-min condition is assumed large enough such that $c_{\text{eigen}} C_B > C_{\text{noise}}$.

*** Term (II): Interference Bias.** This term represents the "leakage" of signal from other covariates due to non-orthogonality. Under the **Block-Irrepresentable Condition (Block-IRC)** or weak correlation assumption, the projection of other variables onto $\mathbf{X}_{\Phi,j}$ is bounded. Specifically, using the Cauchy-Schwarz inequality and the estimation consistency on the remaining variables (which holds under the cone condition even if j is missed):

$$\|\text{Term (II)}\|_F \leq \max_{k \neq j} \left\| \frac{1}{N} \mathbf{X}_{\Phi,j}^\top \mathbf{X}_{\Phi,k} \right\|_2 \cdot \sum_{k \neq j} \|\mathbf{B}_k^* - \hat{\mathbf{B}}_k\|_F.$$

The term is of the order $O(\text{correlation} \times \sqrt{s \frac{\log p}{N}})$. Provided the design is sufficiently incoherent (Block-IRC), this interference is strictly smaller than the primary signal $\|\mathbf{B}_j^*\|_F$.

3. The Contradiction Now consider the KKT inequality (30). The RHS (Penalty Threshold) is:

$$\lambda_g \hat{w}_{g,j} = \lambda_g (\|\tilde{\mathbf{B}}_j\|_F + \tau_N)^{-\gamma_g}.$$

Since $j \in \mathcal{S}^*$, by Assumption 6, the initial estimator is consistent, so $\hat{w}_{g,j} = O_p(1)$ (bounded). Furthermore, the assumption $\sqrt{N} \lambda_g \rightarrow \infty$ is balanced by the decay of the weight such that $\lambda_g \hat{w}_{g,j} \ll \sqrt{\frac{\log p}{N}}$ (or specifically, it is small enough compared to the signal). More formally, for adaptive Lasso, we typically have $\lambda_g \hat{w}_{g,j} \ll \|\mathbf{B}_j^*\|_F$.

Combining these, we have:

$$\text{LHS} \geq \underbrace{c_{\text{eigen}} \|\mathbf{B}_j^*\|_F}_{\text{Signal}} - \underbrace{\text{small bias}}_{\text{Bias}} - \underbrace{\text{noise}}_{\text{Noise}} \approx O\left(\sqrt{\frac{\log p}{N}}\right).$$

$$\text{RHS} = \lambda_g \hat{w}_{g,j} \quad (\text{small}).$$

Because the Beta-min condition ensures the signal dominates noise and bias, and the adaptive weights reduce the penalty for true variables, the inequality:

$$\|\nabla_{\mathbf{B}_j} \mathcal{L}(\hat{\theta})\|_F > \lambda_g \hat{w}_{g,j}$$

holds with high probability. This contradicts the KKT condition (30). Thus, the hypothesis $\hat{\mathbf{B}}_j = 0$ is false, implying $j \in \hat{\mathcal{S}}_{\text{screen}}$. \square

Proof of Theorem 4 (Asymptotic Normality and Valid Inference)

Proof. Let $\mathcal{A} = \mathcal{S}^* \cup \mathcal{C}^{\alpha,*} \cup \mathcal{C}^{\beta,*}$ be the true Oracle active set. By Theorem 2, we have $\mathbb{P}(\hat{\mathcal{A}} = \mathcal{A}) \rightarrow 1$. Hence, our asymptotic analysis is conditioned on the event $\hat{\mathcal{A}} = \mathcal{A}$.

Let $\hat{\boldsymbol{\theta}}_{\mathcal{A}}$ be the restricted estimator. It satisfies the KKT condition:

$$\nabla_{\mathcal{A}} \mathcal{L}(\hat{\boldsymbol{\theta}}_{\mathcal{A}}) + \mathbf{p}'_{\lambda}(\hat{\boldsymbol{\theta}}_{\mathcal{A}}) = \mathbf{0}, \quad (31)$$

where $\mathcal{L}(\boldsymbol{\theta}) = \frac{1}{2N} \|\mathbf{Y} - \mathbf{Z}_{\mathcal{A}} \boldsymbol{\theta}_{\mathcal{A}}\|_2^2$ is the least-squares loss restricted to the active subspace matrix $\mathbf{Z}_{\mathcal{A}}$. Expanding $\nabla_{\mathcal{A}} \mathcal{L}(\hat{\boldsymbol{\theta}}_{\mathcal{A}})$ around the *best spline approximation* $\boldsymbol{\theta}_{\mathcal{A}}^*$ (defined as $\mathbb{E}[\hat{\boldsymbol{\theta}}_{\mathcal{A}}]$ under the unpenalized model):

$$\nabla_{\mathcal{A}} \mathcal{L}(\hat{\boldsymbol{\theta}}_{\mathcal{A}}) = \nabla_{\mathcal{A}} \mathcal{L}(\boldsymbol{\theta}_{\mathcal{A}}^*) + \nabla_{\mathcal{A}}^2 \mathcal{L}(\boldsymbol{\theta}_{\mathcal{A}}^*)(\hat{\boldsymbol{\theta}}_{\mathcal{A}} - \boldsymbol{\theta}_{\mathcal{A}}^*).$$

Note that $\nabla_{\mathcal{A}}^2 \mathcal{L}(\boldsymbol{\theta}_{\mathcal{A}}^*) = \frac{1}{N} \mathbf{Z}_{\mathcal{A}}^{\top} \mathbf{Z}_{\mathcal{A}} := \mathbf{H}_N$. Substituting this into (31):

$$\mathbf{H}_N(\hat{\boldsymbol{\theta}}_{\mathcal{A}} - \boldsymbol{\theta}_{\mathcal{A}}^*) = -\nabla_{\mathcal{A}} \mathcal{L}(\boldsymbol{\theta}_{\mathcal{A}}^*) - \mathbf{p}'_{\lambda}(\hat{\boldsymbol{\theta}}_{\mathcal{A}}).$$

Multiplying by $\sqrt{N} \mathbf{H}_N^{-1}$:

$$\sqrt{N}(\hat{\boldsymbol{\theta}}_{\mathcal{A}} - \boldsymbol{\theta}_{\mathcal{A}}^*) = \underbrace{\sqrt{N} \mathbf{H}_N^{-1} \frac{1}{N} \mathbf{Z}_{\mathcal{A}}^{\top} \mathbf{E}}_{\text{Stochastic Term } (\mathbf{T}_1)} - \underbrace{\sqrt{N} \mathbf{H}_N^{-1} \mathbf{p}'_{\lambda}(\hat{\boldsymbol{\theta}}_{\mathcal{A}})}_{\text{Regularization Bias } (\mathbf{T}_2)}. \quad (32)$$

1. Vanishing Regularization Bias (\mathbf{T}_2) Under Assumption 6 (Oracle Weights), for any $j \in \mathcal{A}$, $\sqrt{N} \lambda \hat{w}_j = o_p(1)$. Since B-splines satisfy the Riesz basis property, the eigenvalues of \mathbf{H}_N are bounded away from 0 and ∞ with probability 1 (Assumption A4). Thus $\|\mathbf{H}_N^{-1}\|_2 = O_p(1)$. It follows that:

$$\|\mathbf{T}_2\|_2 = o_p(1).$$

2. Asymptotic Normality of the Functional Estimator We aim to establish the distribution of $\hat{\beta}_j(t) - \beta_j^*(t)$. We decompose the error into stochastic error and approximation error:

$$\hat{\beta}_j(t) - \beta_j^*(t) = \underbrace{\boldsymbol{\phi}(t)^{\top}(\hat{\boldsymbol{\theta}}_j - \boldsymbol{\theta}_j^*)}_{\text{Estimation Error}} + \underbrace{(\boldsymbol{\phi}(t)^{\top} \boldsymbol{\theta}_j^* - \beta_j^*(t))}_{\text{Approximation Bias } r_j(t)}.$$

Considering the normalized error $\sqrt{N}(\hat{\beta}_j(t) - \beta_j^*(t))$:

$$\sqrt{N}(\hat{\beta}_j(t) - \beta_j^*(t)) = \boldsymbol{\phi}(t)^{\top} [\sqrt{N}(\hat{\boldsymbol{\theta}}_j - \boldsymbol{\theta}_j^*)] + \sqrt{N}r_j(t).$$

Step 2a: Handling Approximation Bias. From spline approximation theory (de Boor, 2001), for a function in the Sobolev space W_2^d , the bias satisfies $\sup_t |r_j(t)| = O(M_N^{-d})$. By the **Undersmoothing Assumption** ($N M_N^{-2d} \rightarrow 0$), we have:

$$|\sqrt{N}r_j(t)| \leq C \sqrt{N} M_N^{-d} = C \sqrt{N M_N^{-2d}} \rightarrow 0.$$

Thus, the systematic bias is asymptotically negligible.

Step 2b: CLT for the Stochastic Term. Let $\mathbf{v}_t = \mathbf{H}_N^{-1} \boldsymbol{\phi}_{full}(t)$ be the projection vector such that the stochastic term for the function is $\frac{1}{\sqrt{N}} \mathbf{v}_t^\top \mathbf{Z}_A^\top \mathbf{E} = \frac{1}{\sqrt{N}} \sum_{i=1}^N (\mathbf{v}_t^\top \mathbf{z}_i) \epsilon_i$. This is a sum of independent random variables with mean 0. We verify the Lindeberg-Feller condition. Given the bounded eigenvalues of B-splines and sub-Gaussian errors, the variance of this scalar sum stabilizes to $\sigma_j^2(t)$. By the Central Limit Theorem:

$$\frac{\boldsymbol{\phi}(t)^\top (\hat{\boldsymbol{\theta}}_j - \boldsymbol{\theta}_j^*)}{\text{sd}(\hat{\beta}_j(t))} \xrightarrow{d} \mathcal{N}(0, 1).$$

3. Consistency of Variance Estimation The plug-in variance estimator is

$$\hat{\sigma}_j^2(t) = \hat{\sigma}_\epsilon^2 \boldsymbol{\phi}(t)^\top (\mathbf{Z}_A^\top \mathbf{Z}_A)^{-1} \boldsymbol{\phi}(t).$$

Since $\hat{\boldsymbol{\theta}}$ is consistent, $\hat{\sigma}_\epsilon^2 \xrightarrow{p} \sigma_\epsilon^2$. Also, $\frac{1}{N} \mathbf{Z}_A^\top \mathbf{Z}_A \xrightarrow{p} \boldsymbol{\Omega}$. Therefore, the ratio of estimated standard error to the true standard deviation converges to 1:

$$\frac{\hat{\sigma}_j(t)}{\sigma_j(t)} \xrightarrow{p} 1.$$

Combining Steps 1, 2a, 2b, and 3, and applying Slutsky's Theorem, we obtain:

$$\frac{\hat{\beta}_j(t) - \beta_j^*(t)}{\hat{\sigma}_j(t)} \xrightarrow{d} \mathcal{N}(0, 1).$$

This completes the proof. \square

B Appendix B: Computational Implementation of Slope Fusion (Hierarchical Strategy)

As detailed in Section 2.6, the generalized AJL objective (10) theoretically incorporates a slope-fusion penalty λ_f^β to detect structural changepoints in the covariate effects $\beta_{jk}(t)$. This capability is clinically relevant for identifying when a biomarker's effect undergoes abrupt changes (e.g., a risk factor becoming relevant only after a certain disease duration).

However, simultaneously solving for variable selection (Group Lasso) and effect segmentation (Slope Fused Lasso) for all p covariates in the ultra-high-dimensional regime is computationally burdensome. Therefore, as discussed in Remark 2, we implement this via a hierarchical regularization strategy.

In the primary screening phase (Algorithm 1), we set $\lambda_f^\beta = 0$ to identify the active set $\mathcal{S} = \{j : \|\hat{\mathbf{B}}_j\|_F > 0\}$. Subsequently, as a post-selection refinement, we solve the following reduced optimization problem restricted to the active set $j \in \mathcal{S}$:

$$\min_{\mathbf{A}, \{\mathbf{B}_j\}_{j \in \mathcal{S}}} L_N(\cdot) + \lambda_f^\alpha \sum_{k=1}^K \sum_{m=1}^{M-1} \hat{w}_{f,km}^\alpha |\Delta a_{k,m}| + \lambda_f^\beta \sum_{j \in \mathcal{S}} \sum_{k=1}^K \sum_{m=1}^{M-1} \hat{w}_{f,jkm}^\beta |\Delta b_{jk,m}| \quad (33)$$

where $\Delta b_{jk,m} = b_{jk,m+1} - b_{jk,m}$. In this step, the group penalty λ_g is typically relaxed or removed to focus on unbiased structural estimation.

This two-stage approach effectively reduces the computational complexity of the fusion step from $O(p)$ to $O(|\mathcal{S}|)$. Model selection between the smooth-slope specification ($\lambda_f^\beta = 0$) and the piecewise-constant-slope specification ($\lambda_f^\beta > 0$) can be guided by the high-dimensional Bayesian Information Criterion (HBIC) (Wang et al., 2007).